

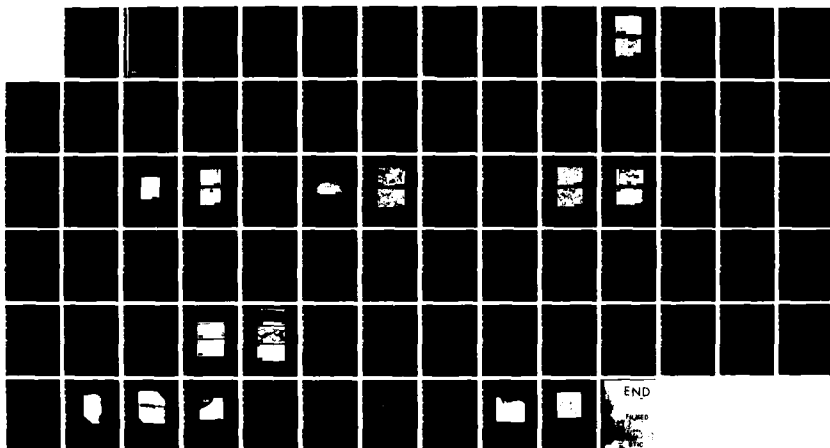
AD-A145 668

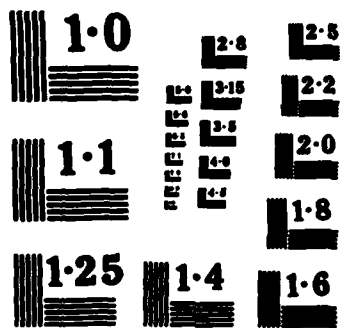
SILICON NITRIDE JOINING(U) SRI INTERNATIONAL MENLO PARK 171  
CA S M JOHNSON ET AL. MAY 84 AFOSR-TR-84-0778  
F49620-81-K-0001

UNCLASSIFIED

F/G 11/2

NL





AD-A145 668

**SILICON NITRIDE JOINING**

Annual Report

May 1984

By: Sylvia M. Johnson and David J. Rowcliffe

Prepared for:

AIR FORCE OFFICE OF SCIENTIFIC RESEARCH (AFOSR)  
Department of the Air Force  
Bolling Air Force Base, DC 20322

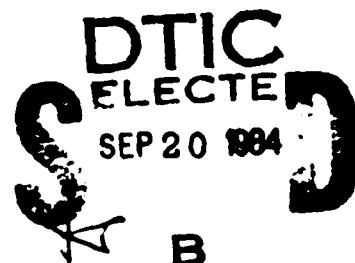
Attention: Capt. J. Hagar  
Program Manager  
Electronic and Material Sciences

Contract No. F49620-81-K-0001  
SRI Project PYU-2527

DTIC FILE COPY



SRI International  
333 Ravenswood Avenue  
Menlo Park, California 94025  
(415) 326-6200  
TWX: 910-373-2046  
Telex: 334 486



84 09 17 009

Unclassified

SECURITY CLASSIFICATION OF THIS PAGE

## REPORT DOCUMENTATION PAGE

1a. REPORT SECURITY CLASSIFICATION <b>Unclassified</b>			1b. RESTRICTIVE MARKINGS		
2a. SECURITY CLASSIFICATION AUTHORITY			3. DISTRIBUTION/AVAILABILITY OF REPORT  <b>Unlimited distribution</b>		
2b. DECLASSIFICATION/DOWNGRADING SCHEDULE			4. PERFORMING ORGANIZATION REPORT NUMBER(S)  <b>PYU-2527, Annual Report</b>		
5. MONITORING ORGANIZATION REPORT NUMBER(S)  <b>AFOSR-TR-</b>			6a. NAME OF PERFORMING ORGANIZATION  <b>SRI International</b>		
6b. OFFICE SYMBOL (If applicable)			7a. NAME OF MONITORING ORGANIZATION  <b>Air Force Office of Scientific Research</b>		
6c. ADDRESS (City, State and ZIP Code) <b>333 Ravenswood Avenue Menlo Park, CA 94025</b>			7b. ADDRESS (City, State and ZIP Code) <b>Department of the Air Force Bolling Air Force Base, DC 20322</b>		
8a. NAME OF FUNDING/SPONSORING ORGANIZATION <b>Air Force Office of Scientific Research</b>			8b. OFFICE SYMBOL (If applicable)		
8c. ADDRESS (City, State and ZIP Code) <b>Department of the Air Force Bolling Air Force Base, DC 20322</b>			9. PROCUREMENT INSTRUMENT IDENTIFICATION NUMBER <b>Contract F49620-81-K-0001</b>		
10. SOURCE OF FUNDING NOS.			11. TITLE (Include Security Classification) <b>Silicon Nitride Joining</b>		
PROGRAM ELEMENT NO.			PROJECT NO.		
TASK NO.			WORK UNIT NO.		
12. PERSONAL AUTHOR(S) <b>Johnson, Sylvia M., and Rowcliffe, David L.</b>					
13a. TYPE OF REPORT <b>Annual</b>		13b. TIME COVERED <b>FROM 2-1-83 to 3-31-84</b>		14. DATE OF REPORT (Yr., Mo., Day) <b>May 1984</b>	
15. SUPPLEMENTARY NOTATION		15. PAGE COUNT <b>74</b>			
17. COSATI CODES			18. SUBJECT TERMS (Continue on reverse if necessary and identify by block number)		
FIELD	GROUP	SUB GR.	Silicon nitride, joining, oxide glasses, oxynitride glasses, vaporization, mechanical properties		
11	02				
19. ABSTRACT (Continue on reverse if necessary and identify by block number) The results obtained in the third year of a continuing investigation into a method of joining silicon nitride with an oxide glass are described. Mechanical behavior of joints at room temperature and the criteria for strong joints are detailed. (Appendix A). Two approaches were taken to strengthen the joints: heat treatments to crystallize the glass in the joint and surface preparation. The high temperature behavior of various $\text{Si}_3\text{N}_4$ glass systems was investigated by means of high temperature mechanical tests, mass spectrometry, theoretical calculations, and mass transport studies. (Appendix B). Alkali and alkaline earth species present in $\text{Si}_3\text{N}_4$ or in the glass were found to be deleterious to joint integrity. The results of all transmission electron microscopy studies performed are included as Appendix C to this report.					
20. DISTRIBUTION/AVAILABILITY OF ABSTRACT <b>UNCLASSIFIED/UNLIMITED <input checked="" type="checkbox"/> SAME AS RPT. <input type="checkbox"/> DTIC USERS <input type="checkbox"/></b>			21. ABSTRACT SECURITY CLASSIFICATION		
22a. NAME OF RESPONSIBLE INDIVIDUAL <b>Capt. J. Hagar</b>			22b. TELEPHONE NUMBER (Include Area Code) <b>202-767-4908</b>		22c. OFFICE SYMBOL <b>NE</b>

DD FORM 1473, 83 APR

EDITION OF 1 JAN 73 IS OBSOLETE.

Unclassified  
SECURITY CLASSIFICATION OF THIS PAGE

# SCIENTIFIC CONTRIBUTIONS

The project leader is David J. Rowcliffe. Studies of the mechanical and high temperature behavior of the joint system were performed by Sylvia M. Johnson. Mass spectrometry studies were conducted by Robert D. Brittain and the theoretical calculations were performed by Robert H. Lamoreaux. TEM studies were performed by Martha L. McCartney at Stanford University under the supervision of Robert Sinclair.

Accession For	
NTIS GRA&I	<input checked="" type="checkbox"/>
ETIC TAB	<input type="checkbox"/>
Unannounced	<input type="checkbox"/>
Justification	
By _____	
Distribution/	
Availability Codes	
Dist	Avail and/or Special
A-1	

AD-700

Card, Technical Information Administration

## INTRODUCTION

Structural ceramics have a wide variety of potential uses that range from low temperature, relatively low stress applications in wear resistant parts to high temperature, high stress applications in advanced heat engines. However, before the full potential of ceramics can be realized, new or improved methods of fabricating components and systems must be developed. Methods of joining ceramics are of particular interest, especially for applications where a joint must have a high strength at high temperature. Silicon nitride is being considered for use in the most demanding applications, and thus a method of reliably joining  $\text{Si}_3\text{N}_4$  is required.

SRI International has devised a new method of joining  $\text{Si}_3\text{N}_4$  that is based on the controlled reaction between an oxide glass and  $\text{Si}_3\text{N}_4$  and has been investigating the method and the system under AFOSR sponsorship. The results obtained during the third year of this investigation are presented in this report.

During the first two years a simple, pressureless method of joining  $\text{Si}_3\text{N}_4$  was developed. Research during the first year<sup>1</sup> concentrated on determining the joining procedure, the range of joining conditions, and TEM studies of the interfacial region. During the second year<sup>2</sup> the joining procedure was refined with the addition of a glazing step, and the mechanical behavior at room temperature was investigated. The joints have strengths at room temperature that are substantially higher

---

<sup>1</sup>R. E. Loehman, M. L. McCartney, and D. J. Rowcliffe, "Silicon Nitride Joining," AFOSR Annual Report, Contract F49260-81-K0001, February 1982.

<sup>2</sup>S. M. Johnson and D. J. Rowcliffe, "Silicon Nitride Joining," AFOSR Annual Report, Contract F-49620-81-K0001, March 1982.

than any previously reported.<sup>3</sup> The mechanisms of fracture and requirements for strong joints are understood. The strength is constant over a range of joining conditions (1575°-1650°C and 30-60 minutes) and is independent of the nitrogen overpressure. The joint thickness determines the joint microstructure, which in turn, determines the strength. Maximum strength, ~ 460 MPa, is achieved with joints that are 20-30  $\mu$ m thick. The explanation of the strengthening mechanism in joined  $\text{Si}_3\text{N}_4$  was the starting point for the research of the third year.

---

<sup>3</sup>P. F. Becher and S. A. Halen, "Solid-State Bonding of  $\text{Si}_3\text{N}_4$ ," Bulletin, of The American Ceramic Society 58, 584-486 (1979).

## TECHNICAL PROGRESS

Progress during the third year of the program is summarized below. The experimental procedures are discussed in more detail in Appendices A and B.

Research during the third year had two objectives: first to investigate the high temperature behavior and, second, to strengthen existing joints. Initially, bend tests were performed in air at temperatures up to 1300°C on  $\text{Si}_3\text{N}_4$  joined with a  $\text{MgO-Al}_2\text{O}_3\text{-SiO}_2$  glass, HN-9M, and with an yttrium oxynitride glass, SG-14. However, the strength of joined bars tested under these conditions was very low. Joints that were originally up to  $\sim 60 \mu\text{m}$  thick expanded to  $\sim 1 \text{ mm}$ . This expansion destroyed the integrity of the joint and the bars fell apart under their own weight. The joint expansion was worst in the samples that were joined with the oxynitride glass. The glass in these joints bubbled extensively and ran out of the joint onto the side of the bar.

Two approaches were taken to improve the strength of the joints. First, an additional step was added to the joining method to ensure that the joints were uniform. Strength depends on joint thickness, and a uniform joint thickness is desirable for controlled strength (see Appendix A). All surfaces were either lapped or polished flat before joining. Second, the samples were heat treated after joining to promote crystallization in the joint. Crystallization treatments were performed in  $\sim 200 \text{ kPa N}_2$  at 1100°-1300°C for 1-2 hours. The strength of heat-treated samples was  $\sim 50\%$  that of nonheat-treated samples. Examination of the fracture surfaces of heat-treated samples indicated that large voids had formed during the heat treatment, so that the glass phase was present as "islands" rather than as the original complete layer. A



complete discussion of the joining parameters and their effect on mechanical properties is given in Appendix A.

The results of the high temperature strength measurements and of the crystallization treatments indicated that vaporization and mass transport reactions were occurring. This conclusion was also supported by the observation that joining times of > 90 minutes resulted in joints with very low strengths, or disappearance of the glass and consequently no joint.

A mass spectrometry study was instigated to determine the vaporization behavior of these materials and systems. Mass spectrometry was performed on the glasses, on two grades of  $\text{Si}_3\text{N}_4$ , and on  $\text{Si}_3\text{N}_4$  glazed with the glasses. The results of the mass spectrometry study are presented in detail in Appendix B. The results of the mass spectrometry study in conjunction with some additional experiments in which  $\text{Si}_3\text{N}_4$  and glazed  $\text{Si}_3\text{N}_4$  were heat treated in  $\text{N}_2$  to study mass transport have important implications for joining, sintering, and long-term exposure of  $\text{Si}_3\text{N}_4$  to high temperatures.

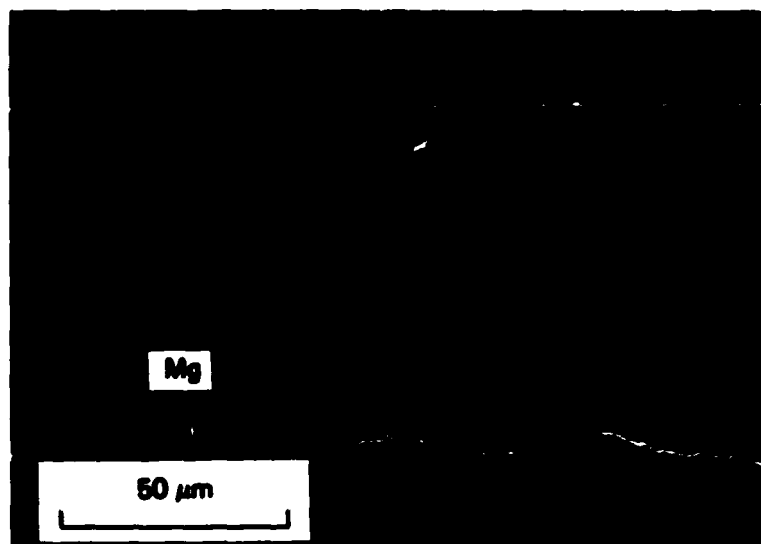
Alkali and alkaline earth species were found to have very high vapor pressures. These species include Mg, which is commonly added as a sintering aid, and impurities such as Na, Ca, and K. The vapor pressures of these elements are significant even when they are only present as impurities. In contrast, amphoteric species, such as Y and Al, were not detected in the vapor. Theoretical calculations indicated a strong dependence of partial pressures of the various species on oxygen potential. In particular, Na, Mg, and SiO have very high vapor pressures under reducing conditions.

Heat treatments were performed on Mg-doped  $\text{Si}_3\text{N}_4$  (NC132) glazed with an  $\text{Y}_2\text{O}_3\text{-Al}_2\text{O}_3\text{-SiO}_2$  glass (SC-14-0) to study mass transport in the system. The appearance of a sample treated for 165 minutes in an overpressure of 6.7 atm of  $\text{N}_2$  at  $1100^\circ\text{C}$  indicated that significant mass transport had occurred. Mg could not be detected in significant amounts in the glass in the sample immediately after glazing. However, after heat treatment an EDAX scan showed that Mg had diffused from the  $\text{Si}_3\text{N}_4$

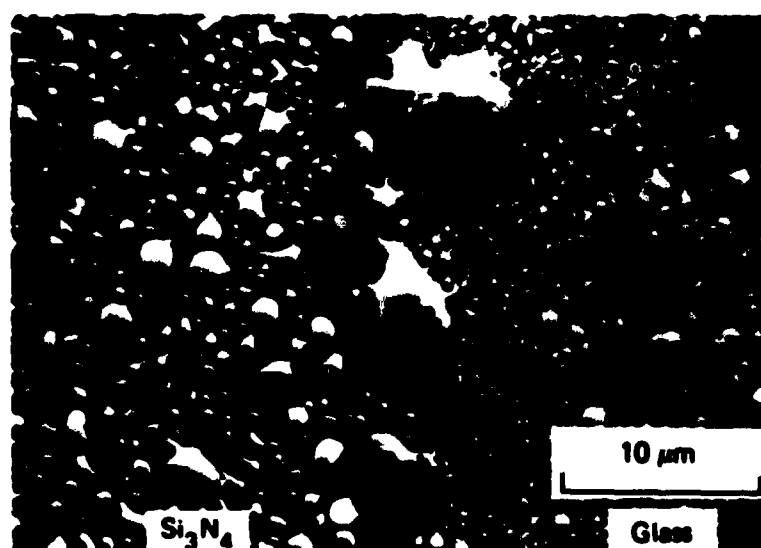
to the outer edge of the glass layer [Figure 1(a)] The surface of the sample, which was polished before the heat treatment, showed considerable evidence of transport from the interior of the  $\text{Si}_3\text{N}_4$  to the interface and to the surfaces of both the  $\text{Si}_3\text{N}_4$  and the glass [Figure 1(b)]. Large globules of a glassy phase exuded from the interface, and smaller exudates were present on the surfaces of the  $\text{Si}_3\text{N}_4$  and the glass. Examination of the interior of the glazed region revealed the presence of bubbles in the glass similar to those observed in mass spectrometry samples (see Appendix B).

The evidence from the high temperature strength measurements, mass spectrometry, theoretical calculations and mass transport studies indicates that mass transport is a serious problem in systems that contain alkali or alkaline earth oxides. Mass transport and the associated vaporization cause degradation of the surface, glass- $\text{Si}_3\text{N}_4$  interface, and the joint. Mass transport to the surface or to the glass will occur regardless of the atmosphere because the interior of the  $\text{Si}_3\text{N}_4$  is very much more reducing than any glass or surface. An important conclusion is that joining systems that contain alkali or alkaline earth oxides are not suitable for use at high temperatures. However, joints made by this method still have potential for use at temperatures below  $\sim 1000^\circ\text{C}$ .

The results of all the transmission electron microscopy studies performed during the first three years of the program are summarized in Appendix C. This part of the program provided detailed information on several aspects of the microstructures and compositional changes that occur in joints. Energy dispersive spectroscopy was used to determine the compositions of grain boundary phases in NC132, so that joining glasses of similar composition could be made. Reactions between  $\text{Si}_3\text{N}_4$  and glass melts were studied using TEM and X-ray diffraction techniques. These studies demonstrated the formation of  $\text{Si}_2\text{N}_2\text{O}$  at the  $\text{Si}_3\text{N}_4$ /glass boundary and also showed the extent to which the original  $\text{Si}_3\text{N}_4$  surface dissolves during joining. Crystallization of Mg-containing glasses occurs through the precipitation of  $\text{MgSiO}_3$  and spontaneous crystallization was observed in scandium-containing glasses used for tracer experiments.



(a) Mg Scan



(b) Interfacial Region

JA-2827-34

FIGURE 1 EDAX SCANS OF Mg-DOPED  $\text{Si}_3\text{N}_4$  (NC132)  
GLAZED WITH  $\text{Y}_2\text{O}_3\text{-Al}_2\text{O}_3$  GLASS (SG-14-0)  
AFTER HEAT TREATMENT IN 8.7 atm  $\text{N}_2$

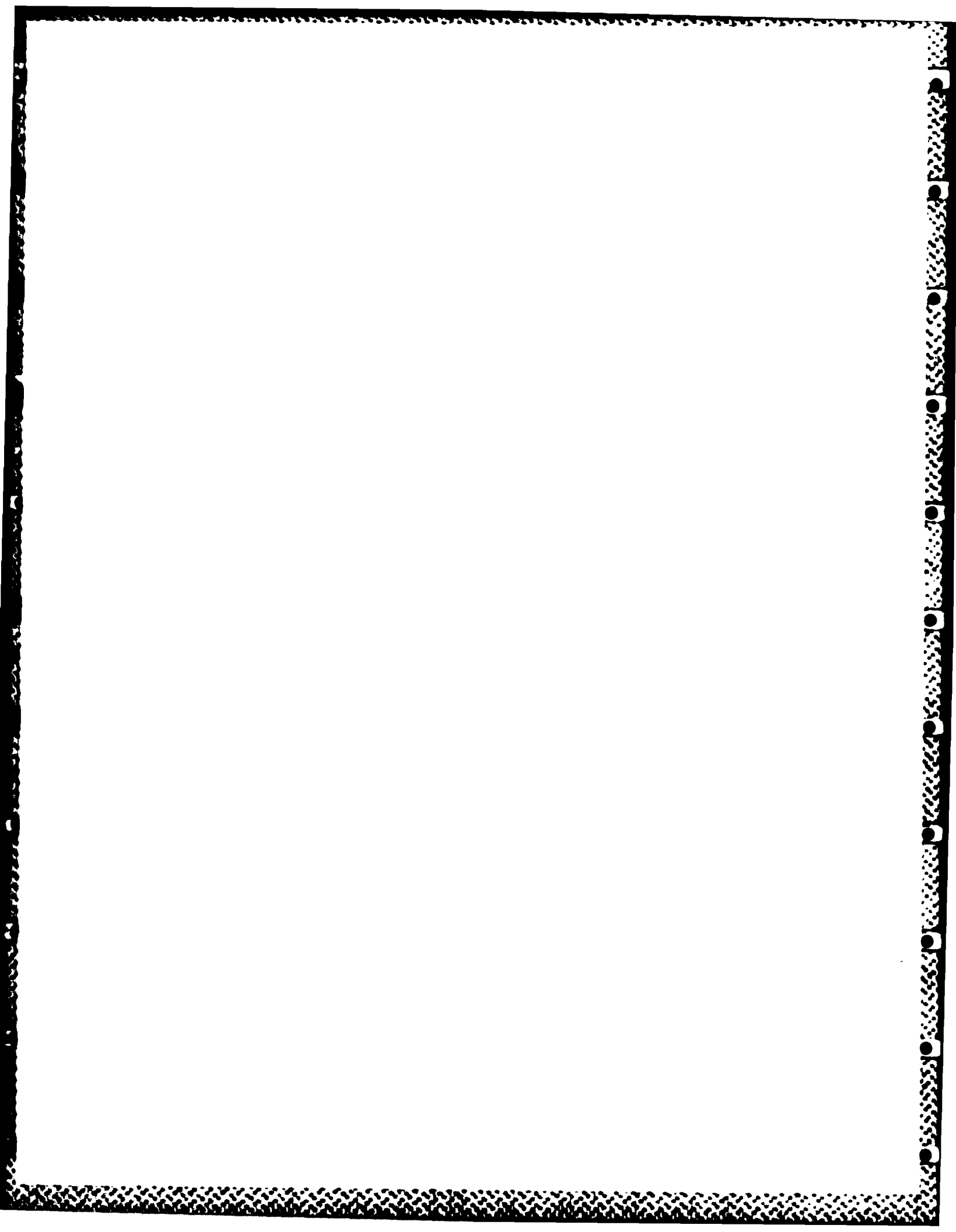
(a) Mg scan across NC132

(b) Interface between NC132 and SG-14-0

## FUTURE WORK

The following research tasks will be undertaken during the fourth year of this research program:

- (1) Optimize the joining glass composition to minimize vaporization. This task entails fabrication of very pure glasses containing less volatile oxide species.
- (2) Investigate the vaporization behavior of several silicon nitrides, including chemical vapor deposited (CVD)  $\text{Si}_3\text{N}_4$  and materials with very low or controlled impurity contents.
- (3) Determine the maximum use temperature of joined ceramics using one or more glasses from Task 1 and a silicon nitride from Task 2. The strength and vaporization behavior at various temperatures up to  $1000^\circ\text{C}$  will be investigated.
- (4) Investigate a method of joining  $\beta\text{-Si}_3\text{N}_4$  coated with thin layers of  $\alpha$ - or amorphous- $\text{Si}_3\text{N}_4$  and oxides. Various combinations of  $\alpha\text{-Si}_3\text{N}_4$ /oxide coatings and the effects of both low and high temperature strengths and fracture mechanisms will be investigated.



## PUBLICATIONS AND PRESENTATIONS

### Publications

1. R. D. Brittain, S. M. Johnson, R. H. Lamoreaux, and D. J. Rowcliffe, "High Temperature Chemical Phenomena Affecting Silicon Nitride Joints," to be published in J. Am. Ceram. Soc., August 1984.
2. S. M. Johnson and D. J. Rowcliffe, "Mechanical Properties of Joined Silicon Nitride," to be submitted to J. Am. Ceram. Soc.

### Presentations

1. S. M. Johnson and D. J. Rowcliffe, "Fracture Mechanisms of Joined Silicon Nitride," Annual Meeting of the American Ceramic Society, Chicago, IL (April 1983).
2. M. L. McCartney, D. B. Marshall, and S. M. Johnson, "Fracture Toughness of Joined  $\text{Si}_3\text{N}_4$ ," Annual Meeting of the American Ceramic Society, Chicago, IL (April 1983).
3. S. M. Johnson and D. J. Rowcliffe, "High Temperature Behavior of Joined Silicon Nitride," Pacific Coast Regional Meeting, American Ceramic Society, San Diego, CA (October 1983).
4. M. L. McCartney, R. Sinclair, and R. E. Loehman, "Properties and Reactivity of Simulated  $\text{Si}_3\text{N}_4$  Grain Boundary Phases," Pacific Coast Regional Meeting, American Ceramic Society, San Diego, CA (October 1983).
5. S. M. Johnson, "Silicon Nitride Joining," Materials Research Seminar, SRI International (March 1984).
6. S. M. Johnson, R. D. Brittain, R. H. Lamoreaux, and D. J. Rowcliffe, "Vaporization Processes in the Joining of Silicon Nitride," Annual Meeting of the American Ceramic Society, Pittsburg, PA (May 1984).

## Appendix A

### MECHANICAL PROPERTIES OF JOINED SILICON NITRIDE

By: Sylvia M. Johnson and David J. Rowcliffe  
SRI International, 333 Ravenswood Avenue,  
Menlo Park, CA 94025

#### ABSTRACT

A technique is described to join  $\text{Si}_3\text{N}_4$  ceramics using oxide glasses. The technique involves a glazing step, followed by a pressureless reaction treatment of 30-60 minutes at  $1575^\circ\text{--}1650^\circ\text{C}$ . The reactions between the glasses and  $\text{Si}_3\text{N}_4$  are reported. An important event is the dissolution of  $\text{Si}_3\text{N}_4$  and the growth of  $\text{Si}_2\text{N}_2\text{O}$  crystals into the joint. The strength of joined bars depends on the joint thickness. Two strength regimes are identified and two corresponding fracture mechanisms are described. A maximum strength of  $\sim 460$  MPa is achieved for joint thickness of  $\sim 30$   $\mu\text{m}$ .

---

This work was supported by the Air Force Office of Scientific Research under Contract F49620-81-K-0001

## I. INTRODUCTION

Until recently, relatively little attention has been paid to joining of ceramic parts to other ceramics or to metals for structural applications. However, the role of ceramics in developing new energy-efficient systems and components has led to a realization of the increasing importance of developing new joining technologies. Potential applications for ceramic/ceramic or ceramic/metal joining include heat engines, heat exchangers and recuperators, and burners.

Joining is important in the fabrication of large structures for two reasons: processing and reliability. Processing of large, complex shapes is both difficult and expensive. Hot pressing is limited to relatively small, simple shapes. Sintering and hot isostatic pressing require an initial forming step, e.g., cold pressing, slip casting, or injection molding, which also restricts the shape and size. Although complex shapes, such as turbine rotors, can be made with these techniques, reliable methods of joining are still required to assemble complete systems.

Reliability of ceramic structures is probably the major concern of manufacturers and users of structural ceramics.<sup>1</sup> Joining smaller pieces to make a large structure might improve reliability. A crack propagating through a monolithic structure can cause catastrophic failure of the entire piece, whereas failure in a joined structure may be limited to one section which can be replaced. Also, the difficulties involved



in processing large, monolithic structures invariably result in larger flaw populations. Smaller pieces may be tested and substandard parts rejected at a much lower cost.

There is no universal method analogous to metallurgical welding for joining two dissimilar or even similar ceramic materials. Brazing with metal alloys that wet  $\text{Si}_3\text{N}_4$  has been used to join  $\text{Si}_3\text{N}_4$ .<sup>2,3</sup> Such joining methods are limited to relatively low use temperatures because the metal alloys used tend to be less refractory and corrosion resistant than the  $\text{Si}_3\text{N}_4$ . Reaction-bonded  $\text{Si}_3\text{N}_4$  has been joined<sup>4</sup> by nitriding a layer of silicon deposited between the parts. The joint formed is porous and the method is not suitable for joining hot-pressed or sintered  $\text{Si}_3\text{N}_4$ . Components have also been fabricated from two pieces by hot pressing with an intermediate powder layer.<sup>5</sup> Becher and Halen<sup>6</sup> hot pressed  $\text{Si}_3\text{N}_4$  pieces using a layer of  $\text{ZrO}_2$  powder and a pressure of less than 1.5 MPa. Room temperature strengths of up to 175 MPa were obtained using this method.

In the work described here, hot-pressed  $\text{Si}_3\text{N}_4$  is joined with an oxide glass. The original concept<sup>7</sup> was based on duplicating the structure of hot-pressed or sintered  $\text{Si}_3\text{N}_4$  where  $\text{Si}_3\text{N}_4$  grains are essentially surrounded and held together by a second phase. This second phase is an oxynitride glass formed by reaction between hot pressing additives (e.g.,  $\text{Al}_2\text{O}_3$ ,  $\text{MgO}$ ,  $\text{Y}_2\text{O}_3$ ) and  $\text{Si}_3\text{N}_4$ . Dissolution of  $\text{Si}_3\text{N}_4$  in the oxide glass used in this work should result in an oxynitride glass with a composition similar to the grain boundary phase in hot-pressed  $\text{Si}_3\text{N}_4$ , and the resulting joint should resemble a large grain boundary.

The actual reactions that occur are slightly more complex than those first envisioned because  $\text{Si}_3\text{N}_4$  dissolves in the glass and silicon oxynitride precipitates. However, such joints are strong at room temperature, and the chemistry of the joint and mechanisms of fracture at room temperature are discussed in this paper. High temperature behavior is discussed elsewhere,<sup>8</sup> as is the detailed chemistry of the glass- $\text{Si}_3\text{N}_4$  reaction.<sup>7,8</sup>

## II. EXPERIMENTAL TECHNIQUES

### (1) Materials

Two billets of hot-pressed  $\text{Si}_3\text{N}_4$  (NC132-I and NC132-II) and one joining composition (HN-9M) were used in most tests. The major impurities in the NC132 billets are listed in Table I. NC132-II was used in most strength tests.

The nominal glass composition (HN-9M), selected to be similar to that found at the grain boundaries of NC132, was as follows:  $\text{SiO}_2$ , 54.97 wt%;  $\text{MgO}$ , 35.27 wt%; and  $\text{Al}_2\text{O}_3$ , 9.66 wt%. The composition of the glass was determined by EDAX and by calculation from the chemical analysis.<sup>9</sup>

### (2) Joining Experiments

The sample configuration used initially consisted of two  $\text{Si}_3\text{N}_4$  plates separated by powdered glass and supported in a boron nitride jig (Fig. 1). This configuration produces a simple end seal. The technique has been refined to a two-stage process: an initial glazing step

followed by the joining operation, which provides more precise control over the joint thickness.

Samples are cleaned in trichlorethylene, acetone, and methanol, and a slurry of the powdered (-100 mesh) glass is applied to one piece. Glazing is performed in a graphite furnace under ~200 kPa  $N_2$ , and temperatures are measured with a Pt-Pt 10% Rh thermocouple. The heat treatment for glazing consists of 15 minutes at 1480°C followed by 10 minutes at 1620°C. This temperature profile resulted in a uniform layer of glass on  $Si_3N_4$ . The glazed end is ground down until only a thin layer of glass remains, and the glazed piece is then placed above an unglazed piece for joining. Although the amount of glass left on the glazed piece depends on the desired joint thickness, it is important that the layer be flat and that the pieces are ground until this condition is reached.

Crystallization treatments were performed on selected joined samples immediately after joining.

### (3) Mechanical Tests

Joined bars were surface ground and cut into bend test bars ~50 mm by 3 mm by 3 mm. Some bars were diamond polished to 1  $\mu m$  on one face, and edges of all bars were bevelled to remove corner cracks. Joint thicknesses were measured in three places in each sample. Samples were broken in a four-point bend configuration, with the polished faces in tension, at a displacement rate,  $\dot{D}$ , of 0.5 mm/min.

#### (4) Microscopy

The joint region in both broken and unbroken bars was examined using SEM. Both the fracture and tensile surfaces of broken bend test bars were studied. Several joint regions were examined by transmission electron microscopy (TEM) and chemically analyzed using an energy dispersive X-ray system (EDAX). The results of the TEM studies on this system are reported elsewhere.<sup>7</sup>

### III. RESULTS

#### (1) Joining Experiments

Examination of the earliest joints produced showed that the thickness of the joined region varied between about 5 and 100  $\mu\text{m}$ , depending on the quantity of glass and the specific joining conditions. Better control of the joining process was achieved when one  $\text{Si}_3\text{N}_4$  piece was glazed.<sup>10</sup> The glazed layer was then ground down to ensure a plane surface and a minimal amount of glass. However, if all the glass on the surface is removed, leaving only the glass that has penetrated the grain boundaries, the pieces do not join. A minimum amount of glass in the joint is therefore necessary for joining because the glass will not flow out of the grain boundaries.

Part of a very thin ( $\sim 5\text{-}\mu\text{m}$ ) joint is shown in Fig. 2. The tungsten particles, which appear as white spots in optical and SEM micrographs and as black spots in TEM micrographs, were analyzed by EDAX and contained W, Si, Fe, Co, Cr, and Mn in varying amounts.<sup>7</sup> Similar particles are found in NCl32 hot-pressed  $\text{Si}_3\text{N}_4$  and are known to

originate from the WC balls used to mill the powders before hot pressing.

Both the glazed layers and the joints contained arrays of cracks normal to the interface; these cracks are caused by differences in thermal expansion coefficients. Silicon nitride has a thermal expansion coefficient,  $\alpha$ , of  $\sim 3.2 \times 10^{-6} \text{ }^{\circ}\text{C}^{-1}$ , whereas HN-9M glass has a thermal expansion coefficient of  $\sim 5.96 \times 10^{-6} \text{ }^{\circ}\text{C}^{-1}$ .<sup>11</sup> The variation in the thermal expansion coefficient of HN-9M glass with  $\text{Si}_3\text{N}_4$  content indicated only a weak dependence of  $\alpha$  on the nitrogen content.<sup>11</sup> The coefficient was reduced to  $\sim 5.2 \times 10^{-6} \text{ }^{\circ}\text{C}^{-1}$  in a glass containing 4.3 at.% nitrogen.

The possibility that this difference in expansion coefficients can cause thermal fracture can be estimated as follows. The strain,  $e$ , developed as a result of the mismatch is:

$$e = \Delta\alpha\Delta T \quad (1)$$

With  $\Delta T \approx 1000 \text{ K}$  and  $\Delta\alpha \approx 2 \times 10^{-6} \text{ }^{\circ}\text{C}^{-1}$ , then  $e \approx 2 \times 10^{-3}$ . The Young's modulus of HN-9M glass was determined by an acoustic resonance technique to be 140 GPa.<sup>7</sup> The stress,  $\sigma_e$ , that develops in the glass as a result of the thermal expansion difference, is thus  $\sim 280 \text{ MPa}$ . The strength of the glass at room temperature was measured to be  $\sim 175 \text{ MPa}$ . Therefore, the thermal expansion mismatch stress is sufficient to cause the observed cracking.

Examples of thermal expansion mismatch cracks are shown in Fig.

3. The cracks are perpendicular to the plane of the joint and develop

in the glass and extend across even very thick joints. Very thin joints,  $< \sim 5 \mu\text{m}$ , are not so extensively cracked. The traces of these cracks can be seen on fracture surfaces where the glass has broken into many small pieces (Fig. 3). The cracks, represented schematically in Fig. 4, extend into the transition zone, which contains a large amount of glass. There are no cracks parallel to the joint because the upper  $\text{Si}_3\text{N}_4$  piece is free to move and relieve any stresses perpendicular to the joint. The glass is not as hard or as tough as the  $\text{Si}_3\text{N}_4$  and tends to chip out along these cracks during grinding. The cracks and their role in the fracture process are discussed in more detail below.

## (2) Glass- $\text{Si}_3\text{N}_4$ Reactions

The reaction between the glass and the  $\text{Si}_3\text{N}_4$  appears to proceed as previously described:<sup>9,11</sup> glass penetrates the  $\text{Si}_3\text{N}_4$  grain boundaries, and  $\text{Si}_3\text{N}_4$  dissolves in the glass. Silicon oxynitride crystallizes from the glass as increasing amounts of  $\text{Si}_3\text{N}_4$  dissolve.

$\text{Si}_2\text{N}_2\text{O}$  crystals were observed using SEM. Figure 5 shows the polished, tensile surface of a broken bend bar. The light crystals growing into the glass from the  $\text{Si}_3\text{N}_4$  are similar to crystals identified as  $\text{Si}_2\text{N}_2\text{O}$  by EDAX.<sup>9</sup> Large glass pockets are also evident in the interfacial region. Tungsten particles, which indicate the original position of the interface, can be seen in the glass above the level of the  $\text{Si}_2\text{N}_2\text{O}$  crystals, indicating the extent of  $\text{Si}_3\text{N}_4$  dissolution.

The interlocking nature of the  $\text{Si}_2\text{N}_2\text{O}$  crystals is shown in Fig. 6, a micrograph of part of the fracture surface through a thin joint. Very little glass remains, and the  $\text{Si}_2\text{N}_2\text{O}$  layer is very porous. This is a

result of the ~12%-15% volume change associated with  $\text{Si}_2\text{N}_2\text{O}$  crystallization and removal of the glass by diffusion along the grain boundaries in the  $\text{Si}_3\text{N}_4$ . The volume change results from the difference in densities between  $\text{Si}_2\text{N}_2\text{O}$ <sup>12</sup> (~2.87 g/cm<sup>3</sup>) and oxynitride glasses<sup>13</sup> (~2.6/cm<sup>3</sup>). As  $\text{Si}_2\text{N}_2\text{O}$  crystals grow, holes form in the surrounding glass. Part of the fracture path through  $\text{Si}_3\text{N}_4$  is also shown in Fig. 6 for comparison.

### (3) Mechanical Tests

Four-point bend tests were used to determine the strength of joints from the first experiments and to define a set of optimum joining conditions. Various glass compositions and two silicon nitrides were used in these initial tests. The joint thickness was not controlled in these early experiments, nor were the test bars polished. The results of the initial strength survey are shown in Fig. 7.<sup>7</sup> Only the maximum strengths obtained are plotted because these represent the best strengths attainable. However, within the optimum range of joining conditions, 1575-1650°C and 30-60 minutes, the strengths are clustered at ~400 MPa and do not appear to depend on the specific joining conditions. Outside the optimum range, the strengths are very low and bars break during normal handling. The strength of  $\text{Si}_3\text{N}_4$  bars is ~725 MPa and of glass bars is ~175 MPa.

Because the maximum strengths appeared to be independent of joining conditions, one set of joining conditions (1580°C for 45 minutes) was chosen for strength tests. Joined bars were polished to 1  $\mu\text{m}$ . Joint thickness can be more easily measured on polished surfaces, and the joint region can be examined by SEM. Several bars were joined under

identical conditions and polished, and their strengths were measured. The fracture and tensile surfaces of several of bars were examined by SEM. The fracture origins were nearly always subsurface, and there was no difference in strength between polished and ground samples.

The fracture strengths, as a function of joint thickness, are plotted in Fig. 8. The shape of the strength-joint thickness curve suggests that there are two fracture mechanisms. The strength increases with joint thickness from joint thicknesses below  $\sim 20$ - $25\text{ }\mu\text{m}$  and decreases with increasing joint thickness above  $\sim 35\text{ }\mu\text{m}$ . The strength is relatively constant within the transition zone of  $\sim 25$ - $35\text{ }\mu\text{m}$ . The maximum strength achieved is  $\sim 460\text{ MPa}$ .

#### IV. DISCUSSION

##### (1) Mechanisms of Fracture

SEM examination of the fracture surfaces indicates that there are indeed two fracture mechanisms corresponding to the two strength regimes. If a joint is very thin,  $< \sim 25\text{ }\mu\text{m}$ ,  $\text{Si}_2\text{N}_2\text{O}$  crystals will grow across the joint and form an interlocking array. However, the glass is consumed during crystal growth, and the resulting structure is very porous, as is shown in Fig. 6. Fracture initiates in the  $\text{Si}_2\text{N}_2\text{O}$  layer, and the crack travels through the  $\text{Si}_2\text{N}_2\text{O}$ , the interface, and the  $\text{Si}_3\text{N}_4$ . The strengths are low as a result of the porosity of the interfacial layer. As the joint thickness increases, more glass will remain between the  $\text{Si}_2\text{N}_2\text{O}$  crystals. An example of the microstructure of a higher strength joint is shown in Fig. 9, where  $\text{Si}_2\text{N}_2\text{O}$  crystals have grown in



the glass. However, some areas are becoming porous as the glass is consumed. The low strength of very thin joints can probably be attributed to incomplete glass coverage of the  $\text{Si}_3\text{N}_4$  and the subsequent formation of large voids in the joint.

Thicker joints,  $> \sim 35 \mu\text{m}$ , contain more glass, and  $\text{Si}_2\text{N}_2\text{O}$  crystals are unable to grow completely across the joint.  $\text{Si}_2\text{N}_2\text{O}$  crystals do grow across the  $\text{Si}_3\text{N}_4$ -glass interface, resulting in a strong interfacial bond. The layer of glass in a thick joint cracks as a result of the thermal expansion mismatch. These cracks run through the interface, but penetrate only a short distance into the  $\text{Si}_3\text{N}_4$ . Large glass pockets are present in the  $\text{Si}_3\text{N}_4$  near the joint,<sup>9</sup> and the cracks extend only into these regions.

The thermal expansion cracks illustrated in Fig. 4, allow the formation of many essentially independent fracture origins. The independent fracture initiation sites are often bubbles or pores in the glass. Cracks grow across each of these areas but stop at the thermal expansion cracks. Eventually, many adjoining areas fracture and catastrophic failure occurs. When a developing crack intersects a preexisting crack, it tends to restart at the ends of that crack and to continue through the  $\text{Si}_3\text{N}_4$ . Higher strengths are associated with a major portion of the crack path running through the  $\text{Si}_3\text{N}_4$ . Figure 10 shows an example of a high-strength sample where the fracture origin is in the glass but the fracture path is mostly through  $\text{Si}_3\text{N}_4$ .

There is a transition region where the two fracture mechanisms occur simultaneously; i.e., some areas of the joint are cracked and others only have  $\text{Si}_2\text{N}_2\text{O}$  crystals present. An ideal joint would have

$\text{Si}_2\text{N}_2\text{O}$  crystals growing across the joint but in a glass matrix. However, a joint microstructure of this type will form only within a very limited joint thickness range; thus, control over the amount of glass used in glazing and joining is critical. However, a range of joint thicknesses for a desired strength can be defined from the present results; i.e., within certain minimum and maximum thickness limits, the joint will have a certain strength regardless of the pertinent fracture mechanism.

## V. CONCLUSIONS

A preliminary survey of joint strength indicated that the strength was independent of the joining time and temperature within the optimum range of 30-60 minutes and  $1575^\circ\text{-}1650^\circ\text{C}$ . Two fracture modes were identified by SEM and linked to the joint thickness and extent of interfacial reaction. The thermal expansion mismatch between the glass and  $\text{Si}_3\text{N}_4$  and the resulting cracks appeared to influence the fracture process greatly. The original concept of forming a thin joint analogous to a grain boundary is not entirely correct because very thin joints are incomplete and weak. Silicon oxynitride crystals, not silicon nitride crystals grow across the joint, forming an interlocking but porous structure. In strong joints, cracks are stopped or deflected into the  $\text{Si}_3\text{N}_4$  by thermal expansion cracks.

The maximum strength achieved is  $\sim 460$  MPa, a substantial fraction of the strength of monolithic pieces. This is the best strength that has been reported for joined  $\text{Si}_3\text{N}_4$ . The method has the added advantage

of being simple and has potential for use as a method of joining  $\text{Si}_3\text{N}_4$  for structural purposes.

#### REFERENCES

- <sup>1</sup>D. J. Rowcliffe and S. M. Johnson "GRI High Temperature Ceramics Workshop," GRI Report, to be published (1984).
- <sup>2</sup>H. R. Heap and C. C. Riley, "Method of Brazing," Brit. Pat. No. 1,310,997, March 21, 1973.
- <sup>3</sup>A. J. Sorrell, "Method of Brazing Ceramic Articles to One Another," Brit. Pat. No. 1,387,478, March 19, 1975.
- <sup>4</sup>R. S. Wilks, "Improvements in or Relating to Joining Silicon Nitride to Silicon Nitrides," Brit. Pat. No. 1,417,169, December 10, 1975.
- <sup>5</sup>M. V. Goodyear and A. Ezis, "Joining of Turbine Engine Ceramics," in Advances in Joining Technology; pp. 113-153. J. J. Burke, A. E. Corum, and A. Tarpinian, Eds., Brook Hill Pub. Co., Chestnut Hill, May 1976.
- <sup>6</sup>P. F. Becher and S. A. Halen, "Solid-State Bonding of  $\text{Si}_3\text{N}_4$ ," Amer. Ceram. Soc. Bull. 58, 584-586 (1979).
- <sup>7</sup>M. L. McCartney, R. E. Loehman, and R. Sinclair, "Silicon Nitride Joining," submitted to J. Am. Ceram. Soc.
- <sup>8</sup>R. D. Brittain, S. M. Johnson, R. H. Lamoreaux, and D. J. Rowcliffe, "High Temperature Chemical Phenomena Affecting  $\text{Si}_3\text{N}_4$  Joining," to be published in J. Am. Ceram. Soc., August 1984.
- <sup>9</sup>R. E. Loehman, M. L. McCartney, and D. J. Rowcliffe, "Silicon Nitride Joining," AFOSR Annual Report, Contract F49620-81-K0001, February 1982.
- <sup>10</sup>R. E. Loehman, Private Communication.
- <sup>11</sup>S. M. Johnson and D. J. Rowcliffe, "Silicon Nitride Joining," AFOSR Annual Report, Contract No. F49620-81-K0001, March 1983.
- <sup>12</sup>I. Idrestedt and C. Broseett, Acta Chem. Scand. 18[8] 1879-1886 (1964).

<sup>13</sup>R. E. Loehman, "Basic Research on Oxynitride Glasses," Final Report prepared for U.S. Army Research Office, Contract No. DAAG-29-79-C0007, July 1982.

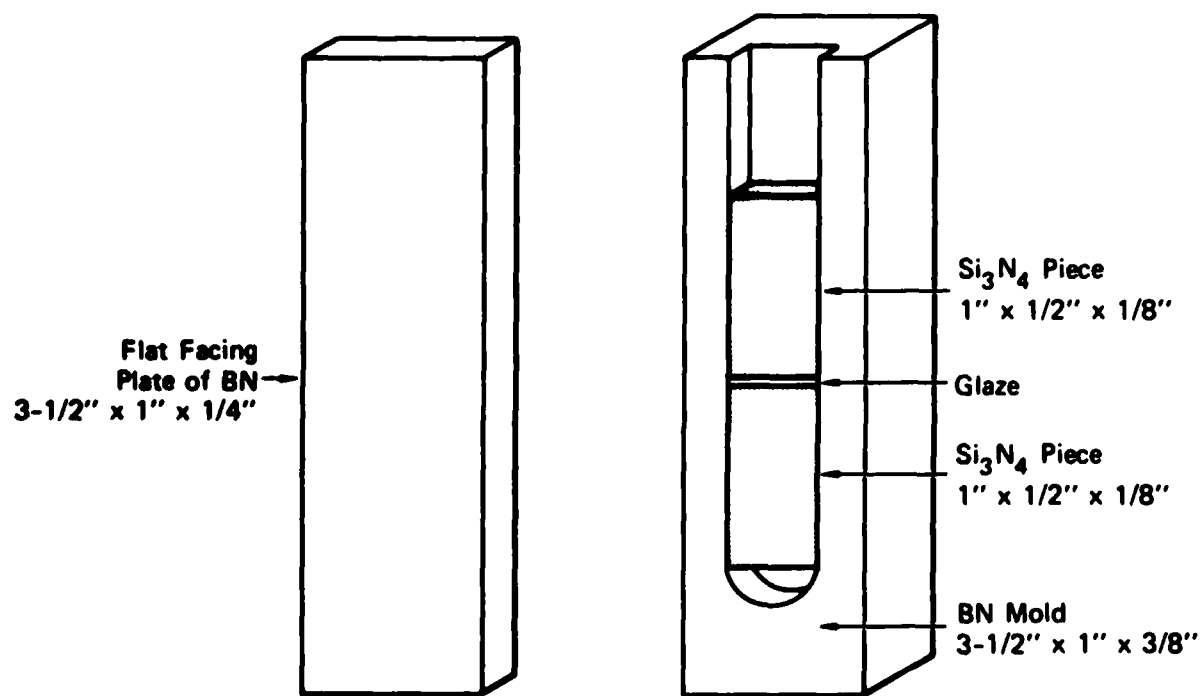
Table I. Major Impurities in Hot Pressed Silicon Nitride<sup>a</sup>

<u>Si<sub>3</sub>N<sub>4</sub> Billet</u>	<u>Impurities (wt%)</u>					
	<u>Mg</u>	<u>O</u>	<u>W</u>	<u>Al</u>	<u>Fe</u>	<u>Ca</u>
NC132-I <sup>b</sup>	1.25	2.46	4.0	0.15	0.3	0.03
NC132-II <sup>b</sup>	0.75	2.37	3.5	0.12	0.25	0.12

<sup>a</sup>American Spectrographic Laboratories, San Francisco, CA.

<sup>b</sup>Norton Co. Worcester, MA.

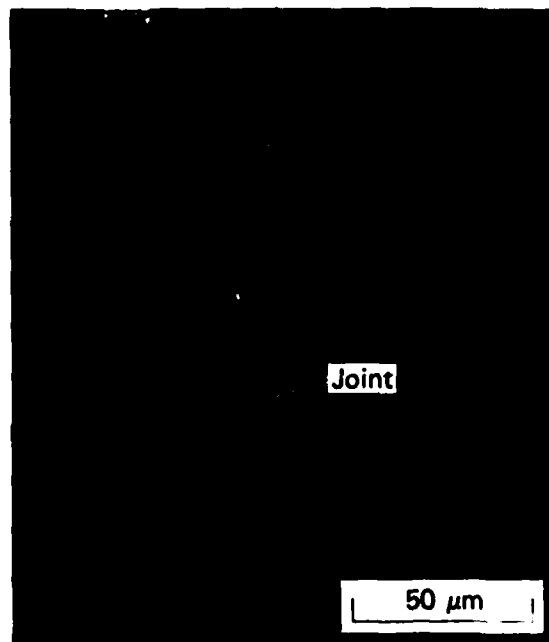
<sup>\*</sup>American Spectrographic Labs, San Francisco, CA.



JA-2527-7

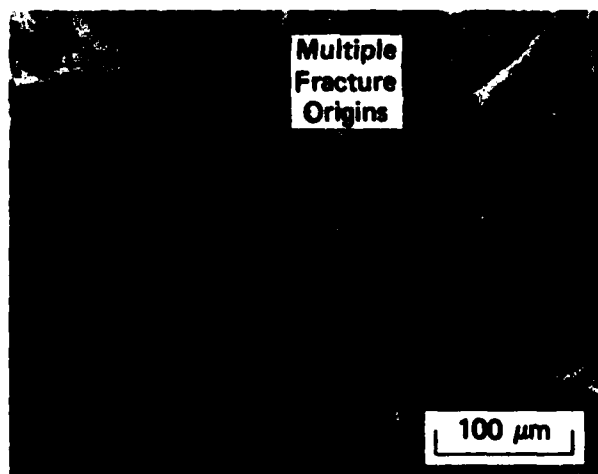
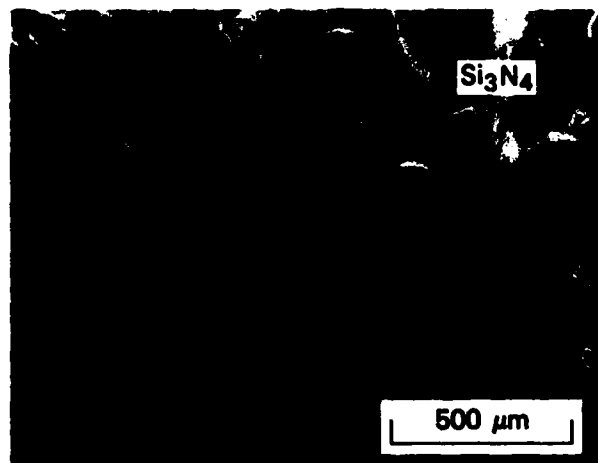
**FIGURE 1 BORON NITRIDE JIG USED IN JOINING TWO PIECES OF Si<sub>3</sub>N<sub>4</sub>**

The upper piece is glazed before being joined to the lower piece.



JP-2527-12

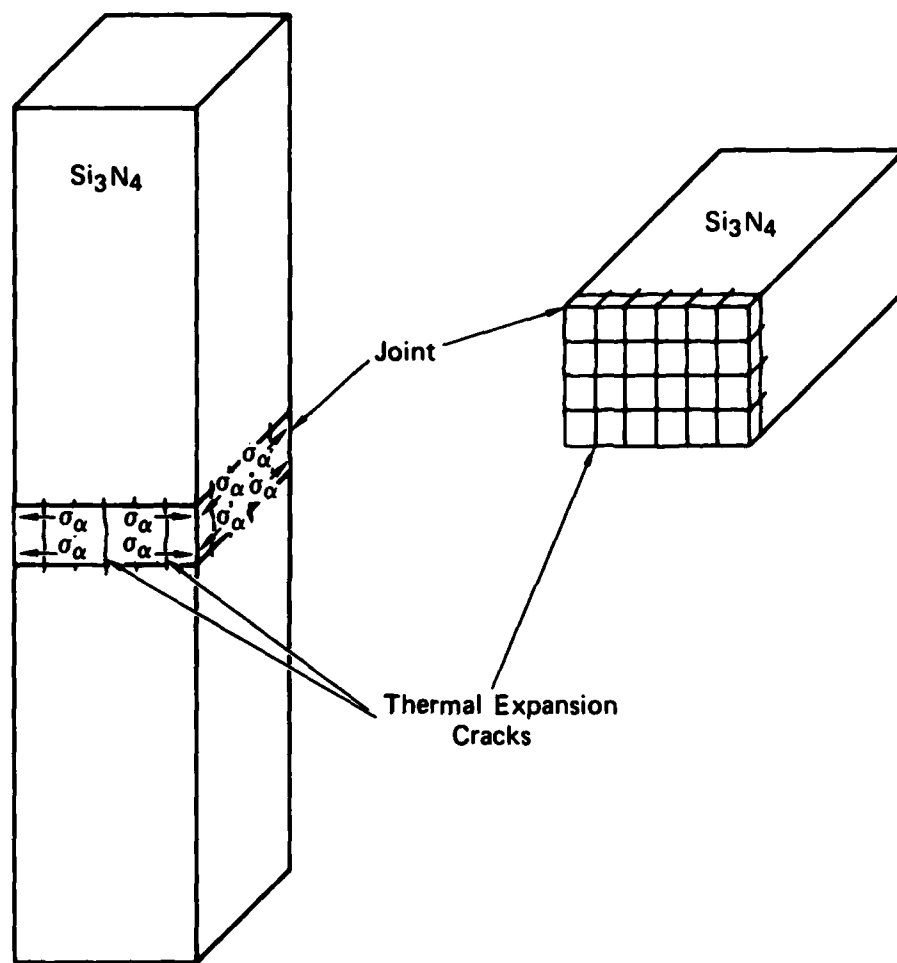
FIGURE 2 OPTICAL MICROGRAPH OF A THIN  
JOINT ( $\sim 5\mu\text{m}$ )



JP-2527-17

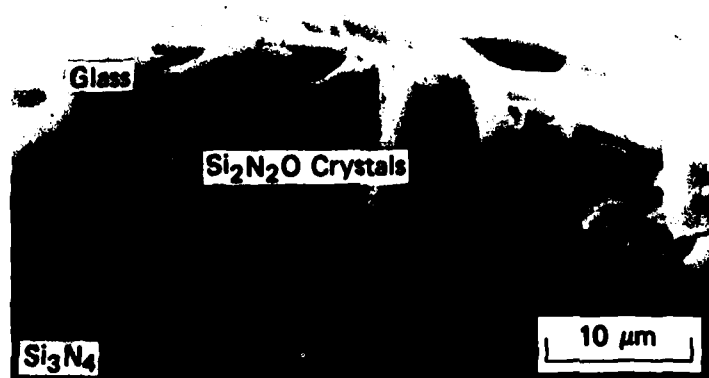
**FIGURE 3 THERMAL EXPANSION CRACKS AND MULTIPLE FRACTURE ORIGINS ON A FRACTURE SURFACE**





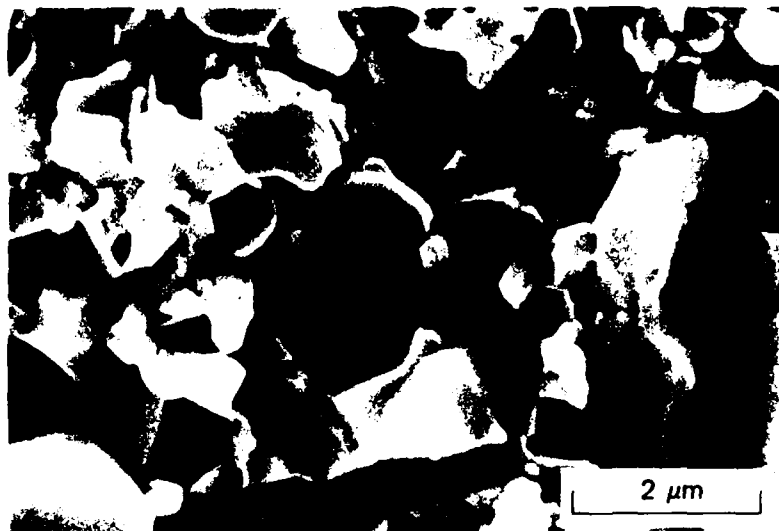
JA-2527-15

FIGURE 4 SCHEMATIC DRAWING SHOWING DEVELOPMENT OF THERMAL EXPANSION MISMATCH CRACKS IN THE JOINT

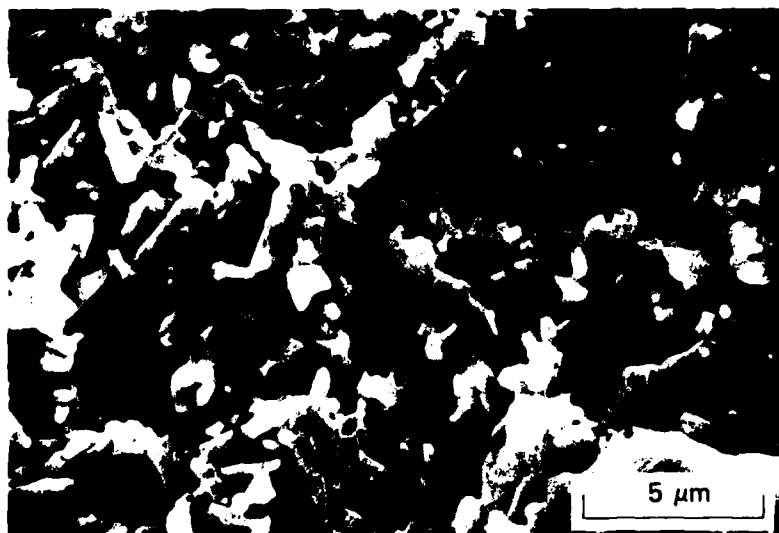


JP-2527-21

FIGURE 5 TENSILE SURFACE OF A BROKEN BEND BAR  
SHOWING Si<sub>2</sub>N<sub>2</sub>O CRYSTALS GROWING INTO  
THE GLASS



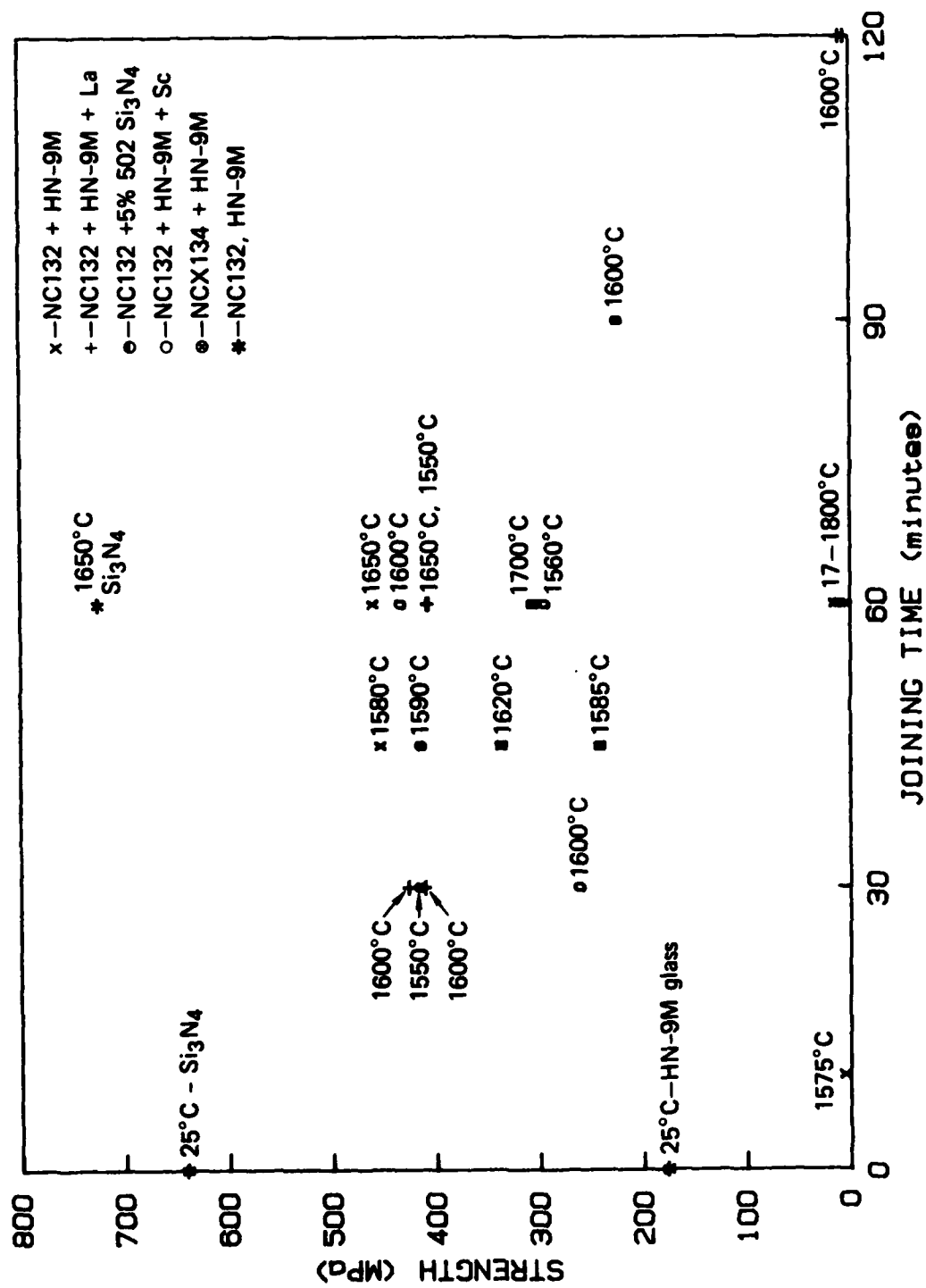
(a) Fracture through  $\text{Si}_3\text{N}_4$



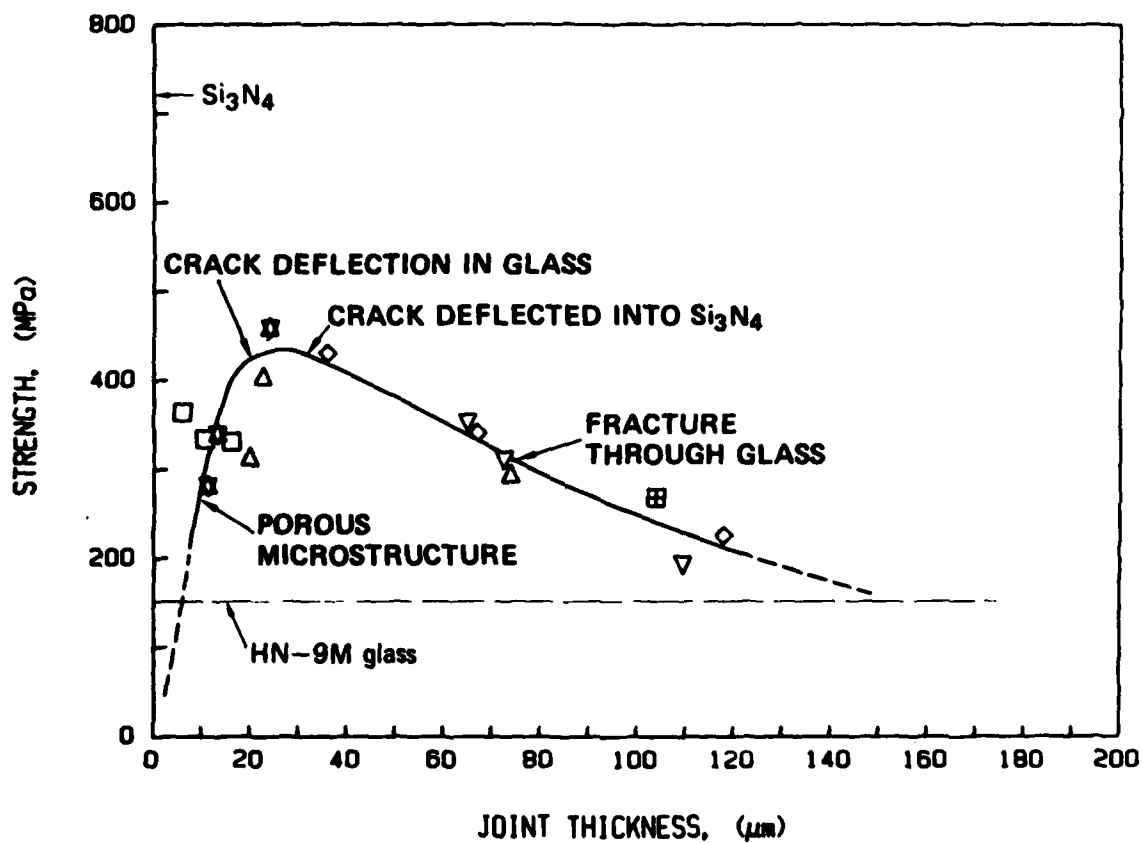
(b) Fracture through interlocking  $\text{Si}_2\text{N}_2\text{O}$  crystals

JP-2527-22

FIGURE 6 FRACTURE SURFACES IN A THIN JOINT.



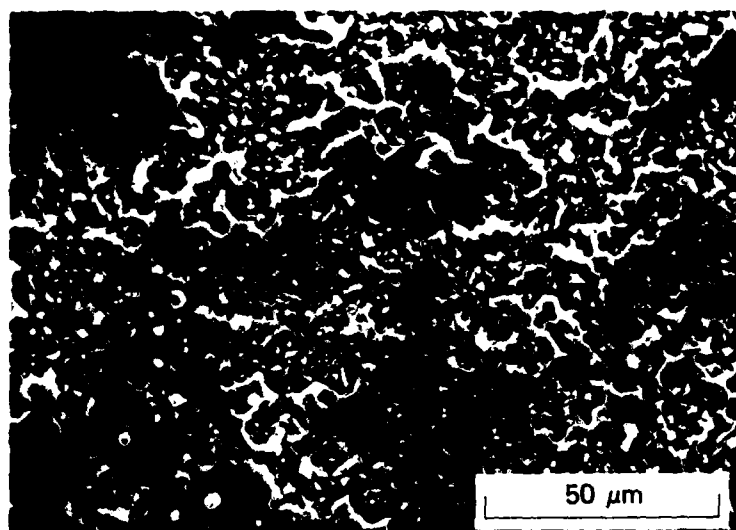
**FIGURE 7 MAXIMUM STRENGTHS OF BARS JOINED UNDER VARIOUS CONDITIONS**



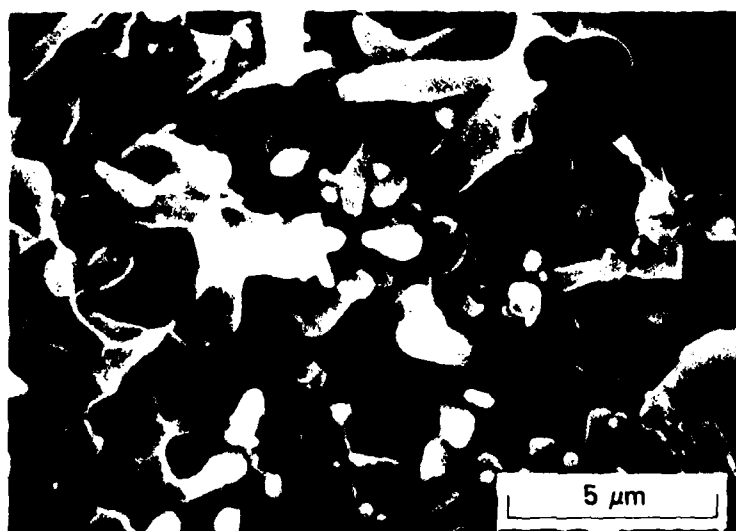
JA-2527-24A

FIGURE 8 STRENGTH VERSUS JOINT THICKNESS

Joining conditions were 1580°C for 45 minutes under 2 atm N<sub>2</sub>.  
Like symbols indicate test bars cut from a single joined specimen.



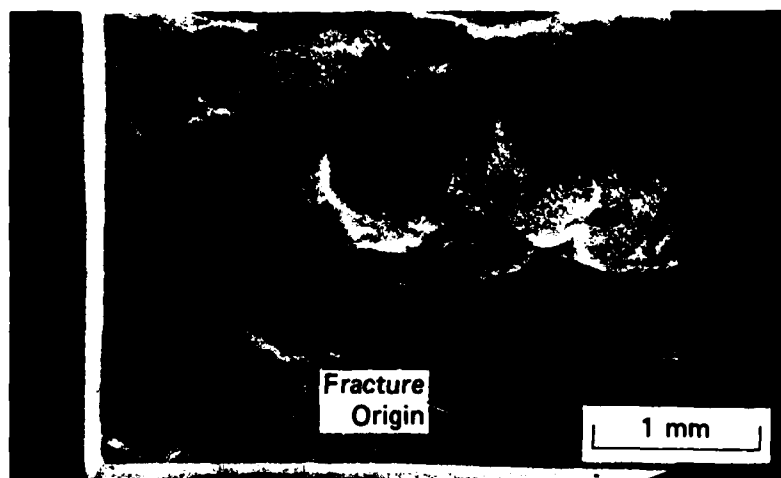
(a)



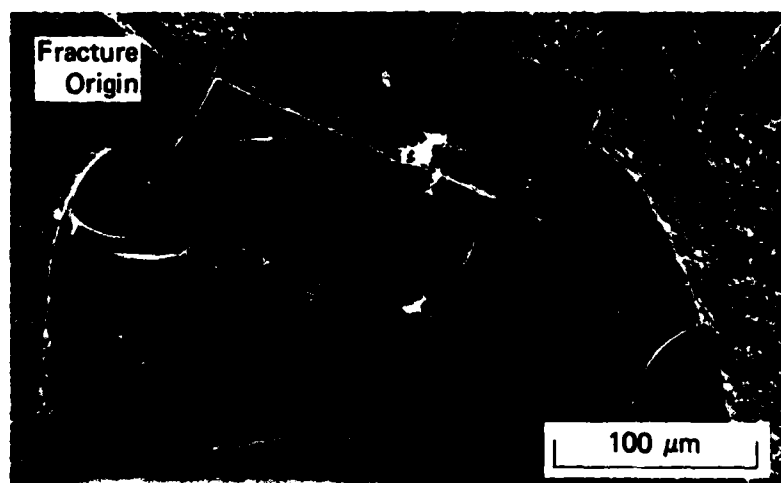
(b)

JP-2527-26

FIGURE 9 MICROSTRUCTURE OF A STRONG THIN JOINT  
SHOWING (a) DEVELOPMENT OF VOIDS IN  
JOINT (b)  $\text{Si}_2\text{N}_2\text{O}$  CRYSTALS IN GLASS



(a)



(b)

JP-2527-27

FIGURE 10 FRACTURE SURFACE SHOWING ORIGIN OF FRACTURE  
IN GLASS AND SUBSEQUENT FRACTURE PATH  
THROUGH  $\text{Si}_3\text{N}_4$

## Appendix B

### HIGH TEMPERATURE CHEMICAL PHENOMENA AFFECTING SILICON NITRIDE JOINTS\*

R. D. Brittain, S. M. Johnson, R. H. Lamoreaux, and D. J. Rowcliffe  
SRI International, 333 Ravenswood Ave., Menlo Park, CA 94025

Knudsen cell mass spectrometry has been employed to study the chemical processes responsible for joint degradation in joined silicon nitride ceramics. Vapor species present above two commercial hot-pressed silicon nitrides and above three joining glasses have been identified, and partial pressures have been estimated at 1480 K. Oxide vaporization products related to reducing conditions were observed. The implications of these results on proposed silicon nitride joining processes are discussed. It appears that oxygen potential gradients within both glazed and unglazed hot-pressed  $\text{Si}_3\text{N}_4$  samples are responsible for the enhanced vaporization rates of the sample and the observed instability of glazed joints at high temperatures. Observed vaporization behavior of oxide additives correlates well with that predicted for the chemically reducing environment of  $\text{Si}_3\text{N}_4$ .

---

\*This work was supported by the Air Force Office of Scientific Research under Contract F49620-81-K-0001.



## I. INTRODUCTION

Reliable methods of joining are required before structural ceramics can be used to full advantage in systems such as the various forms of heat engines. Recently, a method of joining  $\text{Si}_3\text{N}_4$  with an oxide glass was developed<sup>1,2</sup>. The method uses as a joining medium a glass of composition similar to that found as a second phase in hot-pressed or sintered  $\text{Si}_3\text{N}_4$ . Silicon nitride dissolves in the oxide glass that penetrates into the grain boundaries of the bulk material and silicon oxynitride subsequently precipitates as acicular crystals. Ideally, a thin, high strength joint virtually indistinguishable from the bulk material should be formed. This communication describes some aspects of the high temperature behavior, part of an investigation of the chemical and mechanical properties of the system.

The joining method is itself fairly simple. A slurry of powdered glass is applied to one end of a  $\text{Si}_3\text{N}_4$  piece  $\sim 2.5 \times 1.2 \times 0.32$  cm. The piece is placed upright in a mold and heated to  $\sim 1900$  K in 200 kPa  $\text{N}_2$ . The glass forms a thin layer over the end. The glazed piece is then placed above an unglazed piece and heated to  $\sim 1850$ – $1925$  K for 30 to 60 minutes. The joined slab is thus approximately 5 cm long, from which bend bars approximately  $5 \times 0.32 \times 0.32$  cm can be cut.

The room temperature strength and microstructure of the joint region are described elsewhere<sup>2</sup>. The strength is independent of the joining conditions, specifically time and temperature, within an optimum range which is 30 to 60 minutes and  $1850$ – $1925$  K for the NC132 - HN9M system (see Table I for compositions). The strength, however, depends on the joint thickness, with the maximum strength (in four-point-bend)

~ 460 MPa, being achieved with joints ~ 20-30  $\mu\text{m}$  thick. For comparison, the four-point-bend strength of monolithic NCl32 is ~ 725 MPa. The joint strengths are far in excess of those previously reported, the best of these being ~ 175 MPa in a system developed by Becher and Halen<sup>3</sup> which uses  $\text{ZrO}_2$  as a joining material.

The strength at high temperature is of most interest for demanding structural applications such as advanced gas turbines. Four-point-bend test strengths of  $\text{Si}_3\text{N}_4$  joined by oxide and oxynitride glasses were measured in air to 1573 K, but were found to be low. Upon heating, the joints expanded considerably and became porous with a consequent loss of strength.

The room temperature strengths of samples that had been heat treated at 1473-1573 K in ~ 200 kPa  $\text{N}_2$  to promote crystallization in the joint were considerably lower than those of untreated samples, even though crystallization should have resulted in stronger joints. Examination of fracture surfaces by scanning electron microscopy revealed that the glass was no longer present as a uniform layer over the surface, and in some cases was present only as small islands on the  $\text{Si}_3\text{N}_4$ .

The effects observed after high temperature exposure of the joints, namely joint expansion, joint porosity, and incomplete coverage of the joint area, indicated that chemical processes involving mass transport had occurred. Reactions involving significant amounts of mass transport have been observed for hot-pressed  $\text{Si}_3\text{N}_4$  and for glasses similar to the grain boundary phases. For example, Cubicciotti and Lau<sup>4,5</sup> reported

transport of magnesium from the ceramic body to the surface in the oxidation of NCl<sub>3</sub>, an MgO-doped Si<sub>3</sub>N<sub>4</sub>.

Oxynitride glasses volatilize in air at high temperatures, and very high nitrogen pressures are required in their manufacture.<sup>7</sup> The vaporization of gaseous species from Si<sub>3</sub>N<sub>4</sub> and oxynitride glasses has not been studied extensively. Lange<sup>8</sup> and Greskovich and Prochazka<sup>9</sup> investigated volatilization of SiO during sintering of Si<sub>3</sub>N<sub>4</sub> ceramics, but no experimental studies were done on the vaporization behavior of the glass phase components.

We completed a series of experiments to obtain information on chemical processes occurring in joined Si<sub>3</sub>N<sub>4</sub> at high temperature. Knudsen cell mass spectrometry was used to obtain information on vaporization processes relevant to the joint degradation. Vapor species present above glazed Si<sub>3</sub>N<sub>4</sub> samples were identified unambiguously by their threshold ionization potentials and isotope abundance patterns, and partial pressures of each species were measured at ~ 1470-1490 K. A glazed Si<sub>3</sub>N<sub>4</sub> specimen was sectioned and annealed in nitrogen at high temperature, and then examined by scanning electron microscopy and X-ray microanalysis. The influences of impurities, additives, and reactions between glass and Si<sub>3</sub>N<sub>4</sub> upon the mechanical properties of joined silicon nitride have been evaluated in view of known thermodynamic data.

## II. EXPERIMENTAL

Knudsen cell mass spectrometry is a direct sampling technique which identifies the gaseous species present above a condensed phase, alone or in the presence of added gases. The sample is loaded into a Knudsen

cell, a cylindrical holder with an orifice which is a very small fraction of the internal surface area of the cell. This low orifice/cell area ratio leads to conditions approaching equilibrium between vapor and condensed phases within the Knudsen cell. The cell is situated in a high vacuum system so that the orifice is in a line-of-sight with the ion source of a mass spectrometer. Gaseous species effuse from the cell in a collision-free molecular beam that essentially freezes chemical composition; species in the beam are then ionized by electron impact, mass analyzed, and detected by the mass spectrometer. The cell is heated by radiation from a tantalum spiral resistance element, and temperatures are measured by optical pyrometry or by means of a thermocouple. A beam-defining slit, which can be moved over the orifice, permits distinction of cell effusate from ambient gases in the vacuum system. The general experimental technique<sup>10,11</sup> and the quadrupole mass filter<sup>12</sup> apparatus used in these experiments have been described previously.

The samples studied in these experiments are described in Table I. The silicon nitride samples are NC132 (1% MgO)\* and NCX34 (8% Y<sub>2</sub>O<sub>3</sub>)\*; the indicated oxides were added as sintering aids. The surface area of the bulk silicon nitride samples was 1-2 cm<sup>2</sup>. Oxide glasses (HN9M and SG14-0) were prepared by mixing oxide powders (purity >99.5%), melting at 1920 K in air, grinding, and sieving to -100 mesh. The oxynitride

---

\*Norton Co., Worcester, Massachusetts.

glass (SG14) was prepared by adding  $\text{Si}_3\text{N}_4$  to the oxides; this sample was melted under  $\text{N}_2$  at  $\sim 2000$  K before grinding and sieving to -100 mesh.

Each of the separate glasses and silicon nitrides, along with samples of  $\text{Si}_3\text{N}_4$  which were previously glazed at 1900 K with one of the glass samples in accordance with the established joining procedure, was studied by mass spectrometry. Alumina Knudsen cells with 1.5 mm orifices were heated in air at 1500 K before sample loading to remove volatile impurities. The species over each sample were identified from the respective threshold appearance potentials and isotope abundance patterns of the observed ions. The partial pressures of the vapor species were evaluated at 1470-1490 K by measuring each ion intensity,  $I^+$ , at 3 eV above ionization threshold in order to avoid contributions to ion signals by alternative fragmentation processes. The absolute vapor pressure of each species was calculated from the relation

$$P = (kI^+T)/\sigma \quad (1)$$

where  $T$  is the temperature in Kelvins,  $\sigma$  is the relative ionization cross-section, and  $k$  is an instrumental sensitivity constant which was evaluated at specific ionizing energies using gold as a vapor pressure standard. Values for  $\sigma$  were taken from the compilation by Mann;<sup>13</sup> additivity of atomic cross-sections was assumed for molecular ions. The mass discrimination observed in quadrupole filters<sup>14</sup> was minimized by adjusting instrument settings to maximize the signal for  $\text{Au}^+$  before the calibration run. Instrumental settings were held constant following the gold calibration so that instrument sensitivity would be constant.

Signal intensities at approximately 1470-1490 K were studied as a function of time by measuring the mass spectrum at intervals of 1-3 hours. Following mass spectrometry, the interfacial regions of glazed silicon nitride samples were examined by scanning electron microscopy.

A sample of NC132 glazed with SG-14-0 glass was annealed for 2-3/4 hours at 1100°C in an overpressure of N<sub>2</sub> and subsequently scanned by SEM and X-ray analysis to chart any movement of Mg from the Si<sub>3</sub>N<sub>4</sub> into the glass.

### III. RESULTS

#### (1) Mass Spectrometry

Silicon Nitride--A summary of the observed vapor pressures, relative abundances and depletion rates of vapor species above hot-pressed Si<sub>3</sub>N<sub>4</sub> samples containing MgO (NC132) and Y<sub>2</sub>O<sub>3</sub> (NCX34) at 1480 (± 10)K is presented in Table II. The reported pressures of vapor species must be considered as lower limits of those within each sample. The partial pressures observed in the Knudsen cell will be kinetically limited by (1) low surface areas of grain boundary regions of the silicon nitride surfaces and (2) the viscosity of the molten glasses. The metallic elements observed are present in atomic form, as clearly indicated by threshold appearance potentials. Sodium, potassium, and magnesium were observed during the sample heating at temperatures as low as 1200K. The only non-metallic vapor species were SiO and N<sub>2</sub>. We did

not observe Y, Al, W,\* or any compounds containing those metals in the vapor above either silicon nitride sample. Vapor pressures of major species decreased much more rapidly above the NCX34 sample; Na, Mg, and SiO decreased 2-4 times faster in the NCX34 than in NC132, although the level of  $N_2$  remained constant in both samples.

Joining Glasses--Partial pressures of major vapor species above each of the joining glasses at 1490 ( $\pm 10$ )K are reported in Table III. In addition to the reported species, Li, Mn, Fe, Ni, Cu, and Se were observed at low signal levels in HN9M. Fe was the only additional species above SG14 glass, while Cu, Ni, and Li were observed at low pressures above SG14-0.

Glazed Silicon Nitride--Levels of major vapor species above four glazed silicon nitride samples at 1480 ( $\pm 10$ )K are given in Table IV. The minor species were the same as those in the component  $Si_3N_4$  and joining glass samples except that  $N_2$  was no longer observed. Initial Na and K pressures were similar in three of the samples, but were much lower in  $Y_2O_3$  hot-pressed  $Si_3N_4$  (NCX34) glazed with an  $Y_2O_3$ -containing oxynitride glass (SG14). Both Mg and SiO signal levels were significantly higher in samples containing the oxynitride glass. The SiO levels in the NC132 glazed with SG14 were initially more than a factor of three higher than the levels given in Table IV. During this initial phase, "bursts" in the  $SiO^+$  signal were observed; the signal was observed repeatedly to increase sharply before settling back to a stable

---

\*Tungsten-containing particles present in the  $Si_3N_4$  result from WC ball milling and thus tungsten vaporization was of interest.

intermediate level. Signals of other species were stable, and no instability in  $\text{SiO}^+$  signal was observed in other glazed  $\text{Si}_3\text{N}_4$  samples. Although a careful comparison of depletion rates of vapor species in each sample was not undertaken, we did observe gradual depletion of all vapor species in each sample, with the exception that  $\text{SiO}$  evolution above samples glazed with SG14 was almost constant after 1-2 hours.

Microscopy--Figures 1 and 2 show the glazed region of NC132/HN9M and NC132/SG14, respectively, before and after the mass spectrometric measurements. The latter sample exhibited the worst degradation. The glass layers on glazed samples are initially dense and smooth, with the only defects being thermal expansion cracks normal to the interface. After the measurements, the layers were very porous and extensively cracked. The SG14 layer (Fig. 2b) shows the most damage and contains many "bubbles". The large bubbles are most likely due to the decomposition of the oxynitride glass in the vacuum conditions of the mass spectrometer. Figure 2c shows the region close to the interface in the NC132/SG14 sample. The acicular crystals are  $\text{Si}_2\text{N}_2\text{O}$ ,<sup>1</sup> and indicate that, although the glass is damaged, the interface is itself intact. These crystals of  $\text{Si}_2\text{N}_2\text{O}$ , which have been observed in other  $\text{Si}_3\text{N}_4$ /glass systems, are more distinct in NC132/SG14 after the mass spectrometric studies.

## (2) Annealed Specimens

An X-ray microanalysis scan across the interface of an annealed NC132/SG14-0 sample revealed Mg in the glass at distances of up to 60  $\mu\text{m}$  from the interface. As Mg was not originally present in the



glass, this observation indicates that Mg has diffused from the  $\text{Si}_3\text{N}_4$  into the glass. The composition changes at the interface and in the glass are complex and will be the subject of a future paper.<sup>15</sup>

#### IV. DISCUSSION

The present study investigated various phenomena affecting  $\text{Si}_3\text{N}_4$  joints at high temperature. Although the separate observations appear to indicate that the chemistry involved is complex, the results are consistent with the general pattern of  $\text{Si}_3\text{N}_4$  ceramic chemistry that involves equilibria, kinetic factors, oxidation-reduction processes, and silicate solution properties.

Joint degradation at high temperature was characterized by expansion, porosity, and areas from which the joining glass had disappeared; these effects imply that material was being transported to or from the joints. Chemical activity gradients are the driving force for mass transport; a given substance will tend to move toward a region in which it has lower activity. Chemical activity was defined by G. N. Lewis as the ratio of the fugacity of a component to its fugacity in a standard state; for a gaseous component, the fugacity is equal to its partial pressure corrected for gas nonideality.<sup>16</sup> Knowledge of the pressures of gaseous species in equilibrium with condensed phases of different compositions thus enables the prediction of the direction of mass transport, irrespective of whether a condensed phase or gas phase mechanism is involved.

The compounds encountered in the Si-O-N system are  $\text{Si}_3\text{N}_4$ ,  $\text{Si}_2\text{N}_2\text{O}$ , and  $\text{SiO}_2$ . Silicon nitride exposed to relatively high oxygen potentials

develops a surface layer of silica with at most a thin intermediate layer containing silicon oxynitride; exposure at low oxygen pressures produces volatile SiO as a reaction product. In terms of oxidation-reduction chemistry, the bulk of a silicon nitride body, including intergranular phases resulting from use of oxide sintering aids, is a reducing environment when compared to the intermediate oxynitride-rich region and the relatively oxidizing surface silicate phase.

Chemical conditions within the ceramic are dominated by the reducing properties of  $\text{Si}_3\text{N}_4$ , which affect the stability of oxide materials in the intergranular phase. The enhanced vaporization of oxide materials under reducing conditions is well known; MgO, for instance, becomes an unsuitable refractory material because of the evolution of atomic Mg. The chemical activities of oxide components, which are closely related to their vapor pressures, will be higher within  $\text{Si}_3\text{N}_4$  ceramics than under the more neutral or oxidizing conditions found at exposed surfaces of interfaces with glasses of higher oxygen potential. These chemical activity gradients provide a driving force for material transport leading to joint degradation, as well as for phenomena such as the MgO transport observed by Cubicciotti and Lau<sup>4</sup> for NCl32 oxidation. It should be noted that this driving force is in addition to the tendency of components of silicate solutions to achieve uniform distributions under conditions of constant oxygen potential.

Figure 3 shows the partial pressures of principal vaporization species of pure  $\text{Na}_2\text{O}$ ,  $\text{MgO}$ ,  $\text{SiO}_2$ ,  $\text{Al}_2\text{O}_3$ , and  $\text{Y}_2\text{O}_3$  at 1480 K calculated from thermodynamic data<sup>17,18</sup> as a function of oxygen potential. The

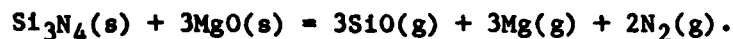
pressures increase as the oxygen potential decreases. Similar plots could be made for other oxides. For a given oxygen potential,  $\text{Na}_2\text{O}$  is more volatile, and  $\text{Al}_2\text{O}_3$  and  $\text{Y}_2\text{O}_3$  are less volatile, than  $\text{SiO}_2$  and  $\text{MgO}$ , which have similar volatilities. In the ceramics, silicate solution effects will lower component activities to some extent, but the general trends will remain the same.

The results of the present study are in excellent agreement with the implications of Figure 3. As seen in Table II, Mg, SiO, and Na are the major vaporization species evolved from both NC132 and NCX34; Mg in NCX34 is notable since it is an impurity rather than an intended constituent. The observed Mg pressure over both ceramic grades is two to three orders of magnitude greater than for congruent vaporization of MgO under neutral conditions. The Na pressure is less than that expected for neutral vaporization, but Na is present as an impurity stabilized in silicate solution in low concentration. In accord with the low volatilities of Al and Y oxides, neither Al nor Y vapor species were observed.

On the basis of concentration and volatility considerations, the SiO, Mg, Na, and K pressures measured over the Y oxynitride glass (SG14) should have been greater than those measured over the Y oxide glass (SG14-0) because of the lower oxygen potential of the oxynitride. This was true for SiO and Mg, but not for Na and K. In all likelihood, significant portions of the small amounts of Na and K initially present as impurities were lost during the preparation of the oxynitride glass. The higher pressures seen for Mg and Na in the magnesia-doped glass (HN9M) probably reflect their greater concentration in these

specimens. The lowest Na and K were observed over NCX34 glazed with SG14 (Table IV), probably reflecting lower amounts in the ceramic and glass. However, the SiO and Mg observed over both NC132 and NCX34 were greater for the oxynitride-glazed specimens, in accord with their lower oxygen potential.

The observation of extensive vaporization of Mg in joints and in commercial grades of  $\text{Si}_3\text{N}_4$  has other implications. Our results are consistent with the reaction:



This behavior explains the relative difficulty of sintering  $\text{Si}_3\text{N}_4$ -MgO powder compacts to high density at atmospheric pressure<sup>19</sup>, compared to hot pressing in which vaporization is suppressed or to pressureless sintering in the  $\text{Si}_3\text{N}_4 - \text{Y}_2\text{O}_3 - \text{Al}_2\text{O}_3$  system.

## V. CONCLUSIONS

The presence of chemical gradients related to oxygen potentials has significant consequences for  $\text{Si}_3\text{N}_4$  joining technology. Considerable chemical transport must be expected for intergranular phase substances if significant chemical activity gradients are present when an oxide glass is used as a joining material. This is in accord with the expansion observed at high temperature for existing joints. Material loss from the joint by vaporization of SiO, Mg, and other volatile species is also expected. Alkali and alkaline earth metal oxide impurities should be minimized in  $\text{Si}_3\text{N}_4$  ceramics, since they will rapidly transport to joints made with oxide glasses.

Joining of MgO hot-pressed silicon nitride with oxide glasses appears to be impractical for high temperature use. On the basis of the lower rates of transport observed in oxidation experiments,<sup>5</sup> joints made with Al<sub>2</sub>O<sub>3</sub> and Y<sub>2</sub>O<sub>3</sub> hot-pressed Si<sub>3</sub>N<sub>4</sub> ceramics should have somewhat better high-temperature performance than that observed for the MgO hot-pressed material. Fabrication of Si<sub>3</sub>N<sub>4</sub> joints with stable high temperature properties will require the elimination of additive concentration and oxidation potential gradients at the joint.

#### References

<sup>1</sup>R. E. Loelman, M. L. McCartney, and D. J. Rowcliffe, "Silicon Nitride Joining", Annual Report, AFOSR, Contract F49620-81-K-0001, February 1982.

<sup>2</sup>S. M. Johnson and D. J. Rowcliffe, "Silicon Nitride Joining", Annual Report, AFOSR, Contract F49620-81-K-0001, March 1983.

<sup>3</sup>P. F. Becher and S. A. Halen, "Solid State Bonding of Si<sub>3</sub>N<sub>4</sub>," Am. Ceram. Soc. Bull. 58 [6] 582-583 (1979).

<sup>4</sup>D. D. Cubicciotti and K. H. Lau, "Kinetics of Oxidation of Hot-Pressed Silicon Nitride Containing Magnesia," J. Am. Ceram. Soc., 61 [11-12] 512-517 (1978).

<sup>5</sup>D. D. Cubicciotti and K. H. Lau, "Kinetics of Oxidation of Yttria Hot-Pressed Silicon Nitride," J. Electrochem. Soc., 126 [10] 1723-1728 (1979).

<sup>6</sup>D. D. Cubicciotti, R. L. Jones and K. H. Lau, "High Temperature Oxidation and Mechanical Properties of Silicon Nitride," Interim Report, AFOSR Contract F44620-76-0116, November 1977.

<sup>7</sup>R. E. Loehman, "Basic Research on Oxynitride Glasses," U. S. Army Research Office, Contract DAAG-29-79-C-007, July 1982.

<sup>8</sup>F. F. Lange, "Volatilization Associated with the Sintering of Polyphase  $\text{Si}_3\text{N}_4$  Materials," J. Am. Ceram. Soc. 65 [8] C-120-C-121 (1982).

<sup>9</sup>C. Greskovich and S. Prochazka, "Stability of  $\text{Si}_3\text{N}_4$  and Liquid Phases During Sintering," J. Am. Ceram. Soc. 64 [7] C-96-C-97 (1981).

<sup>10</sup>D. L. Hildenbrand, "Mass Spectrometric Studies of Bonding in the Group IIA Fluorides," J. Chem. Phys. 48 [8] 3657-3665.

<sup>11</sup>D. L. Hildenbrand, "Dissociation Energies and Chemical Bonding in Alkaline-Earth Chlorides from Mass Spectrometric Studies," J. Chem. Phys. 52 [11] 5751-5759 (1970).

<sup>12</sup>R. D. Brittain and D. L. Hildenbrand, "Catalytic Decomposition of Gaseous  $\text{SO}_3$ ," J. Phys. Chem. 87 [19] 3713-3717 (1983).

<sup>13</sup>J. B. Mann, "Ionization Cross Sections of the Elements Calculated from Mean-Square Radii of Atomic Orbitals," J. Chem. Phys. 46 [5] 1646-1651 (1967).

<sup>14</sup>T. C. Ehlert, "Determination of Transmission Characteristics in Mass Filters," J. Phys. E. 3, 237 (1970).

<sup>15</sup>S. M. Johnson, R. D. Brittain, R. H. Lamoreaux, and D. J. Rowcliffe, "Cation Transport in  $\text{Si}_3\text{N}_4$ /Glass Couples," to be submitted to J. Am. Ceram. Soc.

<sup>16</sup>G. N. Lewis and M. Randall, Thermodynamics, 2nd ed., K. S. Litzer and L. Brewer, Eds. McGraw-Hill, New York, 1961.

<sup>17</sup>D. R. Stull and H. Prophet, JANAF Thermochemical Tables, 2nd ed., NSRDS-NOS37, U.S. Government Printing Office, Washington, DC, 1971, and supplements.

<sup>18</sup>V. P. Glushko, L. V. Gurvich, et al., "Thermodynamic Data for Individual Substances," Vol. 4, Institute for High Temperatures, National Academy of Sciences of the U.S.S.R., Moscow, 1983.

<sup>19</sup>G. R. Terwilliger and F. F. Lange, "Pressureless Sintering of  $\text{Si}_3\text{N}_4$ ," J. Mater. Sci. 10 [7] 1169-1174 (1975).

Table I. Samples Investigated by Mass Spectrometry

Sample	Designation	Nominal Composition (wt %)				
		Mg	Y	W	Al	Fe
MgO Hot-Pressed $\text{Si}_3\text{N}_4$	NC132	0.8	---	1.8	0.2	0.2
$\text{Y}_2\text{O}_3$ Hot-Pressed $\text{Si}_3\text{N}_4$	NCX34	---	5.3	2.1	0.2	0.3
Sample	Designation	Nominal Composition (wt %)				
		MgO	$\text{SiO}_2$	$\text{Al}_2\text{O}_3$	$\text{Y}_2\text{O}_3$	N
MgO Glass	HN9M	35	55	10	---	---
$\text{Y}_2\text{O}_3$ Glass	SG14-0	---	34	20	46	---
$\text{Y}_2\text{O}_3$ Oxynitride Glass	SG14	---	32	19	43	6



Table II. Partial Pressures, Relative Abundances, and Depletion Rates  
of Vapor Species Above  $\text{Si}_3\text{N}_4$  Samples at 1480 K

Vapor Species	Relative Abundance		Pressure (mPa)		Depletion Rate (%/h)	
	NC132	NCX34	NC132	NCX34	NC132	NCX34
SiO	100.0	100.0	317	528	14	43
Mg	100.7	15.9	324	84	13	60
Na	193	10.4	627	55	24	40
K	12.2	1.1	40	6	27	57
$\text{N}_2$	4.1	12.5	13	66	0	0
Mn	8.2	2.7	27	14	20	59
Fe	2.8	0.7	9	4	19	45
Li	0.4	0.3	1.4	1.4	40	33
Ni	0.2	0.3	0.7	1.5	40	0
Se	--- <sup>a</sup>	0.3	---	1.6	---	0
Y	---	---	---	---	---	---
Al	---	---	---	---	---	---
W	---	---	---	---	---	---

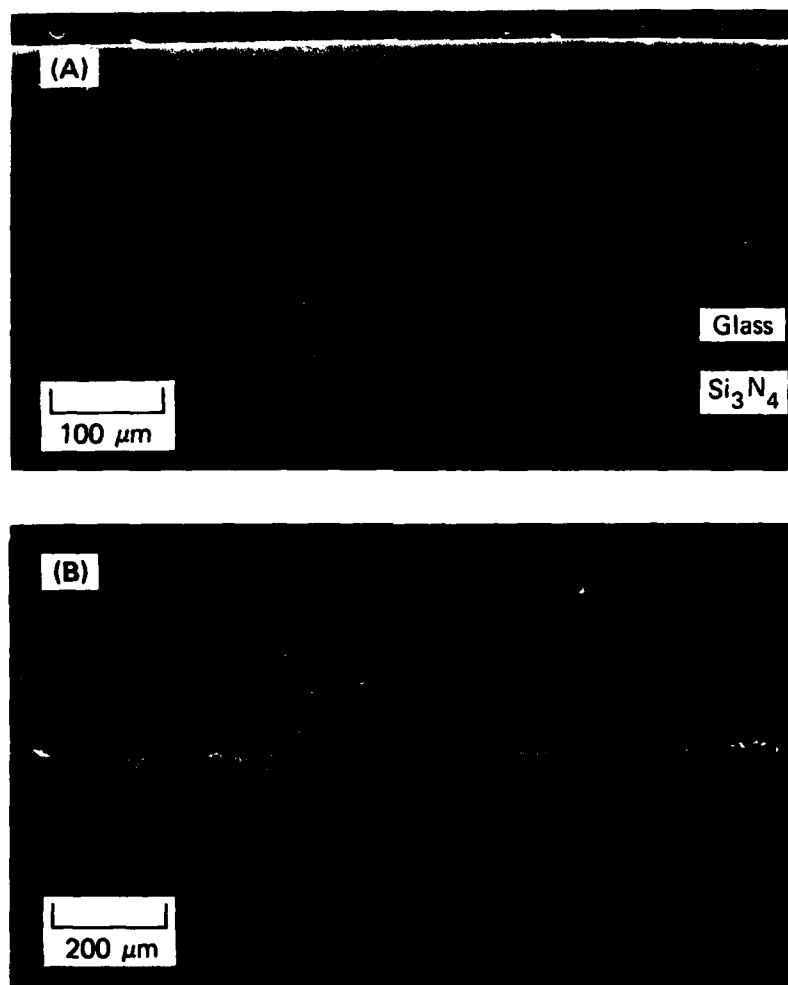
<sup>a</sup> --- indicates Not Detected

Table III. Partial Pressures of Major Vapor Species above  
Joining Glasses at ~ 1490 K

Vapor Species	Partial Pressure (mPa)		
	HN9M	SG14	SG14-0
SiO	99	334	1.3
Mg	8.8	3.7	1.5
Na	331	5.6	76
K	9.3	0.6	7.8

Table IV. Partial Pressures Above Glazed  
 $\text{Si}_3\text{N}_4$  Samples at  $\sim 1480$  K

Vapor Species	Partial Pressure (mPa)			
	NC132+NH9M	NC132+SG14	NCX34+SG14	NCX34+SG14-O
SiO	25	132	58	6.5
Mg	11	48	14	3.2
Na	72	66	13	73
K	1.9	1.9	<0.5	1.9

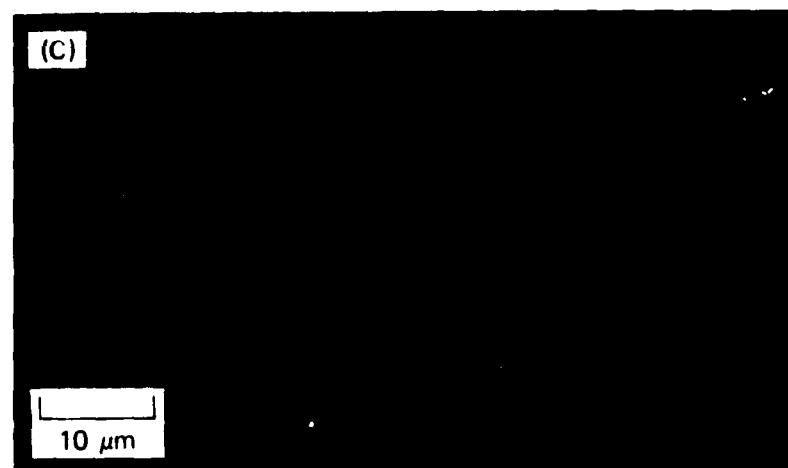
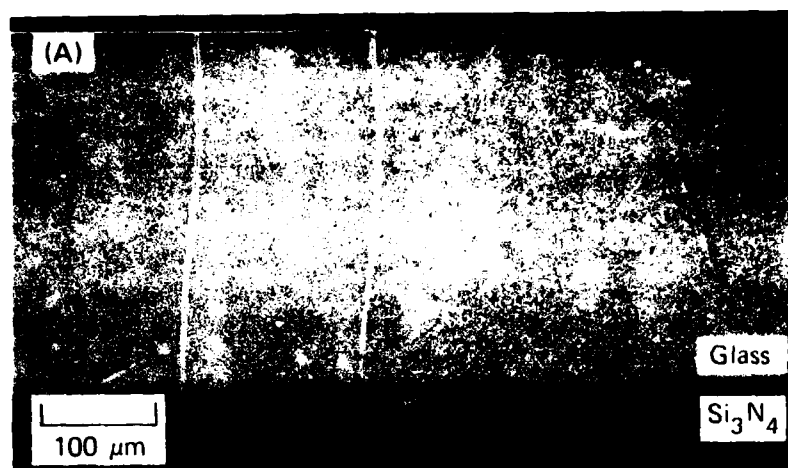


JP-2527-32

FIGURE 1 NC-132 (MgO)  $\text{Si}_3\text{N}_4$  GLAZED WITH MAGNESIA (HN-9M) GLASS

(A) As glazed.

(B) After heating to 1480 K in mass spectrometer.



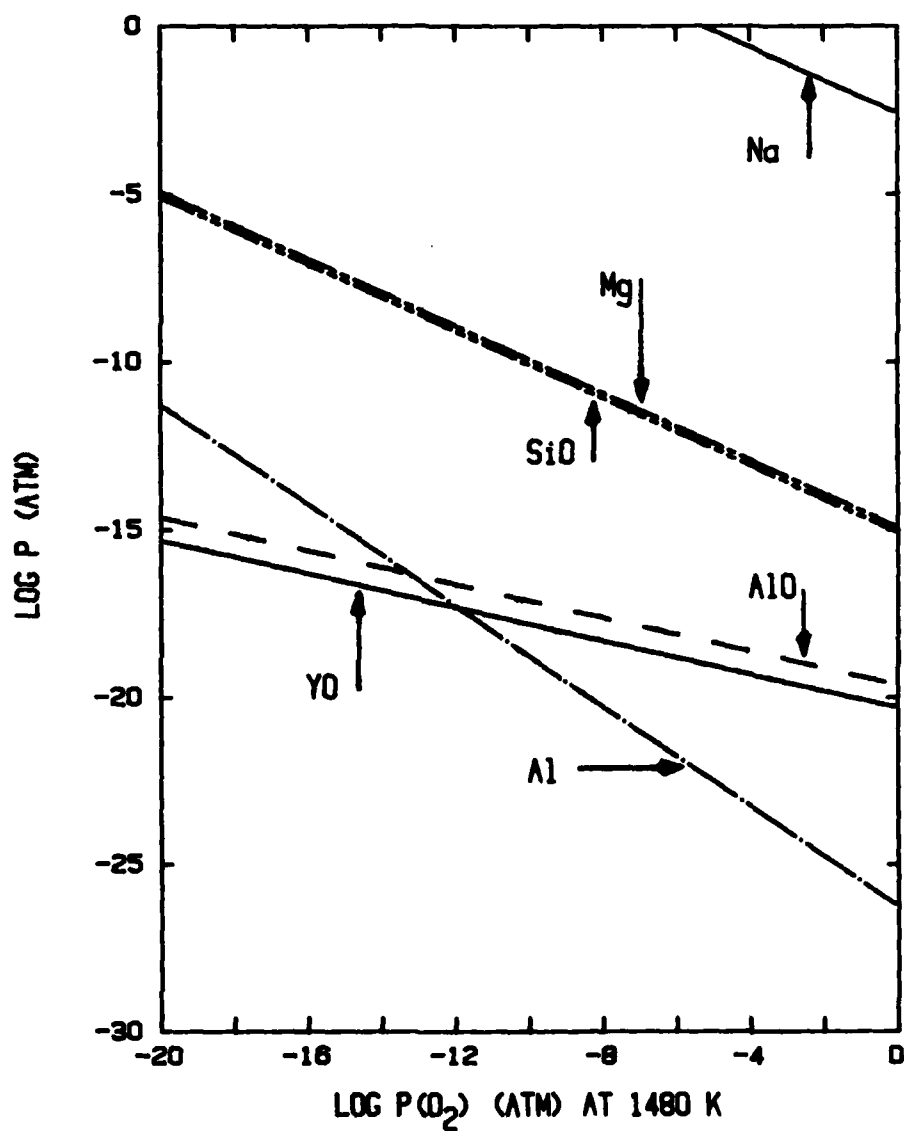
JP-2627-30

FIGURE 2 NC-132 (MgO)  $\text{Si}_3\text{N}_4$  GLAZED WITH YTTRIUM OXYNITRIDE GLASS (SG-14)

(A) As glazed.

(B) After heating to 1480 K in mass spectrometer.

(C) Interfacial region of (B) showing  $\text{Si}_2\text{N}_2\text{O}$  crystals.



JA-2627-33

FIGURE 3 PRESSURES OF PREDOMINANT VAPORIZATION SPECIES OF PURE  $\text{Na}_2\text{O}$ ,  $\text{MgO}$ ,  $\text{SiO}_2$ ,  $\text{Al}_2\text{O}_3$  AND  $\text{Y}_2\text{O}_3$  AS FUNCTIONS OF OXYGEN POTENTIAL AT 1480 K

## Appendix C

### SUMMARY OF WORK COMPLETED

#### RESEARCH ON SILICON NITRIDE JOINING

Stanford Subcontract #SRI C-10383

R. Sinclair, P.I.

This report summarizes the work done by M. L. McCartney on the  $\text{Si}_3\text{N}_4$  joining project during the period of December 1, 1980 through November 30, 1983. A complete description is in preparation and is to be submitted as a Ph.D. thesis for Stanford University. Results from five main areas of the research are presented. These topics include:

1. Comparison of the glass composition used for joining with the grain boundary phase in hot-pressed  $\text{Si}_3\text{N}_4$ .
2.  $\text{Si}_3\text{N}_4$ /glass reactions in melts.
3. The microstructure and mechanical properties of joined  $\text{Si}_3\text{N}_4$ .
4. The effect of dissolved  $\text{Si}_3\text{N}_4$  on the properties of the joining glass.
5. Crystallization behavior.

## GLASS COMPOSITION

The composition of glass (HN-9M) used to join  $\text{Si}_3\text{N}_4$  was 10 wt. %  $\text{Al}_2\text{O}_3$ , 35 wt. %  $\text{MgO}$ , 55 wt. %  $\text{SiO}_2$ . This composition was compared to the grain boundary composition of the host NC132  $\text{Si}_3\text{N}_4$  by two methods. Firstly, an average grain boundary composition was calculated based on cation and oxygen analyses of a bulk piece of NC132  $\text{Si}_3\text{N}_4$  (using the same procedure as Loehman had used for the powder lots). The second technique employed was energy dispersive spectroscopy (EDS) in transmission electron microscopy (TEM) to analyze pockets of glass in the NC132  $\text{Si}_3\text{N}_4$ . The two results are shown on the  $\text{MgO-Al}_2\text{O}_3\text{-SiO}_2$  ternary phase diagram of Fig. 1. The NC132 used in these experiments was most likely made from the powder lot HN-10 since those compositions most closely matched. The lower Al content in the EDS analysis may be due to some small Al solubility in the  $\text{Si}_3\text{N}_4$ . The higher Si content could be from  $\text{Si}_3\text{N}_4$  dissolved in the glass. The HN-9M glass was a reasonable match for the grain boundary phase without nitrogen.

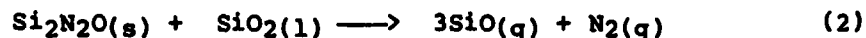
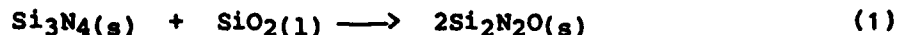
The elastic modulus of the glass, measured using an acoustic resonance technique, was 140GPa.

## $\text{Si}_3\text{N}_4$ Glass Melts

Loehman's work on analyzing the phase reactions of amorphous and  $\alpha\text{-Si}_3\text{N}_4$ /glass melts was continued using  $\beta\text{-Si}_3\text{N}_4$  powders. The powder x-ray diffraction (XRD) results showed that the rate of dissolution for 15 wt. %  $\text{Si}_3\text{N}_4$  in 85% glass were slowest for  $\beta\text{-Si}_3\text{N}_4$ .  $\text{Si}_2\text{N}_2\text{O}$  appeared as an intermediate phase for the melts with both high and low concentration of  $\text{Si}_3\text{N}_4$ . TEM analysis showed lath-like  $\text{Si}_2\text{N}_2\text{O}$  precipitates near dissolving  $\text{Si}_3\text{N}_4$  particles (Fig. 2). The  $\text{Si}_3\text{N}_4$  was inhomogeneously distributed.



It is postulated that the following reactions occurred during the heating of the melts at 1650°C and caused the amount of Si<sub>2</sub>N<sub>2</sub>O to decrease, despite the two atmospheres nitrogen pressure used.



The maximum solubility of Si<sub>3</sub>N<sub>4</sub> in the HN-9M glass was 12 - 15 wt. %. A minimum amount (2.5 wt. % Si<sub>3</sub>N<sub>4</sub>) was needed in order to prevent devitrification of the glass into MgSiO<sub>3</sub>, when cooled in a graphite element furnace at a rate of 44°C/minute.

#### Joined Si<sub>3</sub>N<sub>4</sub>

Four point bend tests were conducted on joined samples, the NC132 Si<sub>3</sub>N<sub>4</sub>, and the HN-9M glass (Results are presented in Fig. 18 of the March 1983 Annual Report). The strengths of the joined samples fell half-way between the strength of the Si<sub>3</sub>N<sub>4</sub> and that of the glass. The strengths did not appear to be correlated to joining times (for 20 min. <T< 120 min) or joining temperature (1550°C <T< 1700°C). Scanning electron microscopy (SEM) was performed on the samples and showed that the fracture path went through both the Si<sub>3</sub>N<sub>4</sub> and the glass. It also indicated the presence of extensive cracks perpendicular to the interface which were probably caused by the thermal expansion mismatch between the glass and the Si<sub>3</sub>N<sub>4</sub>.

TEM of the joined samples showed that Si<sub>2</sub>N<sub>2</sub>O had precipitated out at the interface where the Si<sub>3</sub>N<sub>4</sub> had dissolved away. The original presence of Si<sub>3</sub>N<sub>4</sub> was confirmed by the remaining W-Fe rich impurity particles, which act as markers of the original interface (Fig. 11 in February 1982 Annual Report).

5 wt. %  $\alpha$ - $\text{Si}_3\text{N}_4$  had been added to the joining glass for some experiments, in order to promote the precipitation of  $\text{Si}_2\text{N}_2\text{O}$ . The strengths of these samples were average. Since the solubility of  $\text{Si}_3\text{N}_4$  glass is 15 wt. %, this amount is probably too small to cause extensive reactions. TEM analyses did show increased  $\text{Si}_2\text{N}_2\text{O}$  precipitation near the interface in the glass (Fig. 3). Few W-Fe particles can be seen and so this region was not originally NC132  $\text{Si}_3\text{N}_4$ . The  $\text{Si}_2\text{N}_2\text{O}$  particles did not extend across the interface. Enlarged pockets of glass were found in the  $\text{Si}_3\text{N}_4$  near the interface for all joined samples (Fig. 4).  $\text{Sc}_2\text{O}_3$  and  $\text{La}_2\text{O}_3$  were added to some joining glass for some experiments and used as tracers to determine how far into the  $\text{Si}_3\text{N}_4$  the joining glass diffused. EDS with SEM was tried first but was unsuccessful due to the small concentrations of Sc and La. TEM with EDS analysed discrete pockets of glass and traces of Sc were found as far in as 700  $\mu\text{m}$  (Fig. 8 of March 1983 Annual Report). This gives an approximate diffusion coefficient of  $D = 10^{-6} \text{ cm}^2/\text{sec}$  at 1600°C.

Microindentation was used to correlate the change in microstructure with local changes in mechanical properties. Figures 5 and 6 show that there is a sharp drop in hardness and fracture toughness for the  $\text{Si}_3\text{N}_4$  near the interface (closer than 100  $\mu\text{m}$ ). This region corresponds to the areas where large amounts of glass had been discovered by TEM. The smaller enlarged pockets at distances greater than 100  $\mu\text{m}$  into the  $\text{Si}_3\text{N}_4$  did not degrade the room temperature hardness or fracture toughness.

#### Effect of Dissolved $\text{Si}_3\text{N}_4$ on the Properties of HN-9M Glass

Samples of HN-9M glass and various amounts of  $\text{Si}_3\text{N}_4$  were melted at 1650°C for one hour in a nitrogen atmosphere. As mentioned previously if  $\geq 2.5\%$   $\text{Si}_3\text{N}_4$  was added, crystallization was inhibited. Lesser amounts of  $\text{Si}_3\text{N}_4$  allowed  $\text{MgSiO}_3$  to precipitate. Samples with 2.5 to 15 wt. %  $\text{Si}_3\text{N}_4$

were sent out for determination of the nitrogen concentration by gas fusion reaction. These results, which can err on the low side, indicated that only half of the nitrogen from the dissolved  $\text{Si}_3\text{N}_4$  had remained in the glass. These samples were then used for indentation tests to ascertain the variation in hardness and elastic modulus with nitrogen content. Figures 7 and 8 present the data showing an increase in hardness and modulus with increasing nitrogen concentration. These results agree well with the work on other oxynitride glass systems, which suggest that the nitrogen leads to increased cross linking and a tighter bound glass structure and hence the increase in hardness and modulus [1].

R. E. Loehman of Sandia Labs provided glass transition temperature and thermal expansion measurements. The thermal expansion measurements did not show any systematic decrease with increasing nitrogen content while the glass transition temperature increased from 750°C at 0 at. % N to 850°C at 4 at. % N.

Combining the hardness vs nitrogen concentration data with information about the average hardness of the glass in the joints (found by microindentation), provided a method for determining the nitrogen content of the glass in the joint. According to Figure 7, the nitrogen content was about 4 at. % This nitrogen concentration is within the range of that found by Clarke and Zaluzec in the grain boundary phase of hot-pressed  $\text{Si}_3\text{N}_4$  by using electron energy loss spectroscopy [2]. This is also at the limit of saturation for  $\text{Si}_3\text{N}_4$  in the glass. Chemically, the glass joint indeed did resemble a large angle grain boundary.

#### Crystallization

$\text{Si}_3\text{N}_4$ /glass melts with  $\text{Si}_3\text{N}_4$  concentrations from 5-15% were heat treated at 1300°C for times from 0.5 hours to 2 hours. The results

(Fig. 18 in March 1983 Annual Report) showed predominantly  $\text{MgSiO}_3$  precipitating. The higher was the  $\text{Si}_3\text{N}_4$  content, the longer the sample took to crystallize.

TEM of joined samples heat treated at  $1300^\circ\text{C}$  showed strained particles of  $\text{MgSiO}_3$  and occasionally  $\text{Mg}_2\text{SiO}_4$  (Fig. 9). The strain, indicated by the distorted bend contours, was due to the difference in thermal expansion coefficient and change in density between the glass and the crystalline phases. The pockets of glass were high in Al and Ca (Fig 19 March 1983 Annual Report).

The Sc-HN-9M glass used for the tracer experiments had spontaneously crystallized in certain regions (Fig 10). The crystallites were fine particles which  $2\frac{1}{2}$  D imaging in TEM showed to be close in orientation. Segregation of pockets of glass was not observed, and the crystallized regions had the same Sc-Mg-Al-Si composition as the original glass.

#### REFERENCES

1. R. E. Loehman "Oxynitride Glasses", J. of Non Cryst. Solids 42, 433-446 (1980).
2. D. R. Clarke, N. J. Zaluzec "The Intergranular Phase in Hot-Pressed Silicon Nitride: III, A Refinement of the Elemental Composition", J. Am. Cer. Soc. 65 (8) C-132-133 (1982).

## FIGURE CAPTIONS

- FIGURE 1  $\text{MgO-Al}_2\text{O}_3\text{-SiO}_2$  Phase Diagram  
HN-9 and HN-10 are calculated grain boundary phases for two powder lots of NC132  $\text{Si}_3\text{N}_4$ . HN-9M is the base composition used for joining. NC132 is the calculated grain boundary phase from the bulk  $\text{Si}_3\text{N}_4$ . EDS is the composition obtained by EDS analyses in TEM of glassy pockets in NC132.
- FIGURE 2  $\text{Si}_2\text{N}_2\text{O}$  precipitating near a dissolving  $\beta\text{-Si}_3\text{N}_4$  grain in a  $\text{Si}_3\text{N}_4$ /glass melt with 15%  $\text{Si}_3\text{N}_4$  and 85% glass.
- FIGURE 3  $\text{Si}_2\text{N}_2\text{O}$  precipitates in the glass of a joined sample. 5 wt. %  $\alpha\text{-Si}_3\text{N}_4$  had been added to the glass.
- FIGURE 4  $\text{Si}_3\text{N}_4$  grains surrounded by glass 10  $\mu\text{m}$  away from the interface. The amorphous regions are marked by g.
- FIGURE 5 Variation in hardness as a function of distance into the  $\text{Si}_3\text{N}_4$  away from the  $\text{Si}_3\text{N}_4$ /glass interface.
- FIGURE 6 Variation in fracture toughness as a function of distance into the  $\text{Si}_3\text{N}_4$  away from the  $\text{Si}_3\text{N}_4$ /glass interface.
- FIGURE 7 Variation in hardness with nitrogen content for HN-9M glass.
- FIGURE 8 Variation in elastic modulus with nitrogen content for HN-9M glass.
- FIGURE 9  $\text{MgSiO}_3$  precipitate (indicated by Mg) in the  $\text{Si}_3\text{N}_4$  close to the joint interface. The residual glass high in Al and Ca is marked by G.
- FIGURE 10 Dark field image of a crystallized Sc-Mg-Al-Si phase.





Figure 2





Figure 3

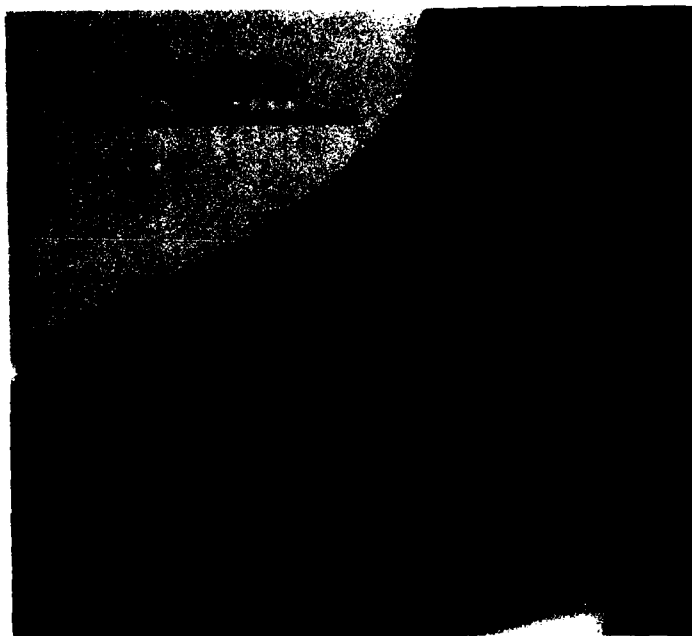


Figure 4

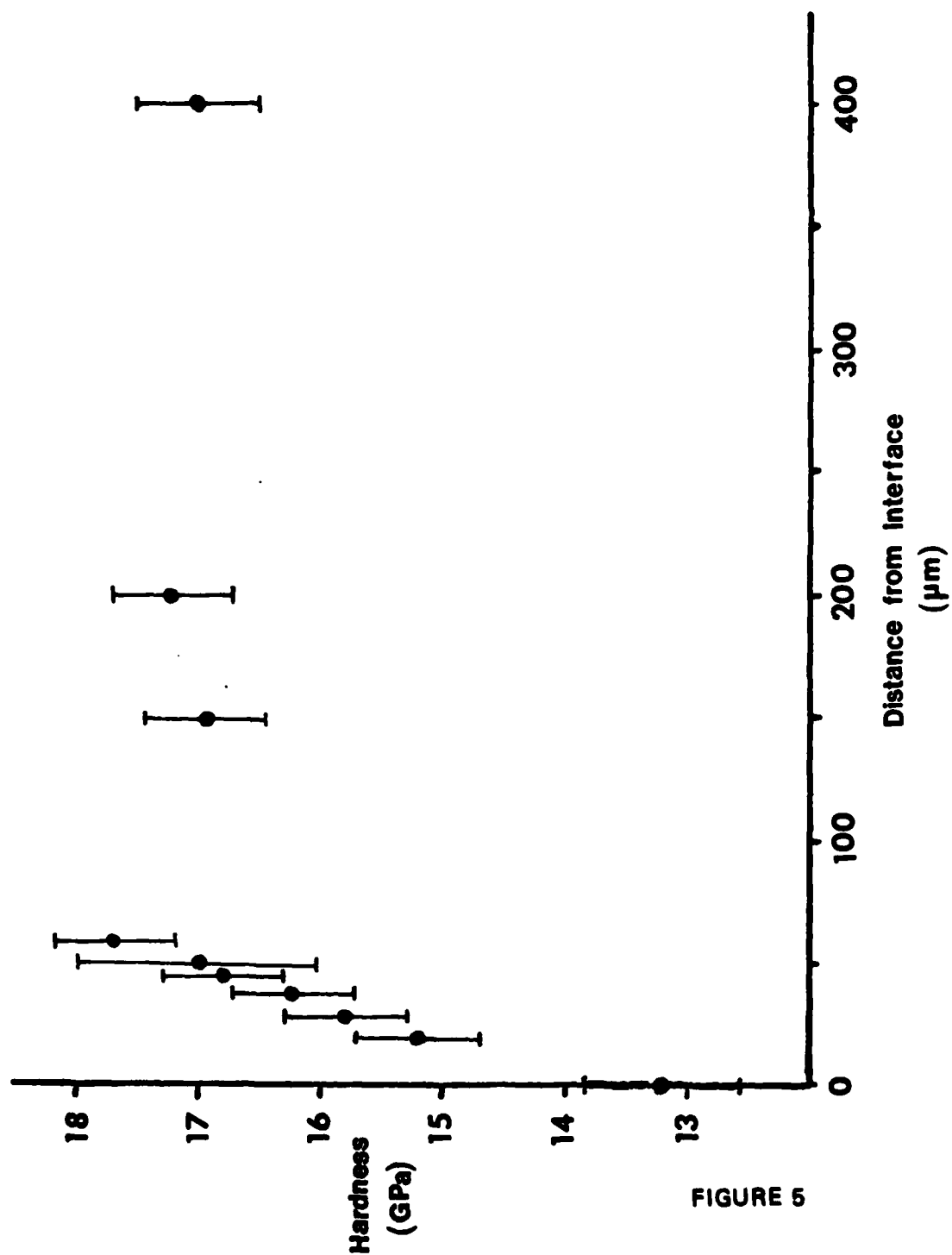


FIGURE 5

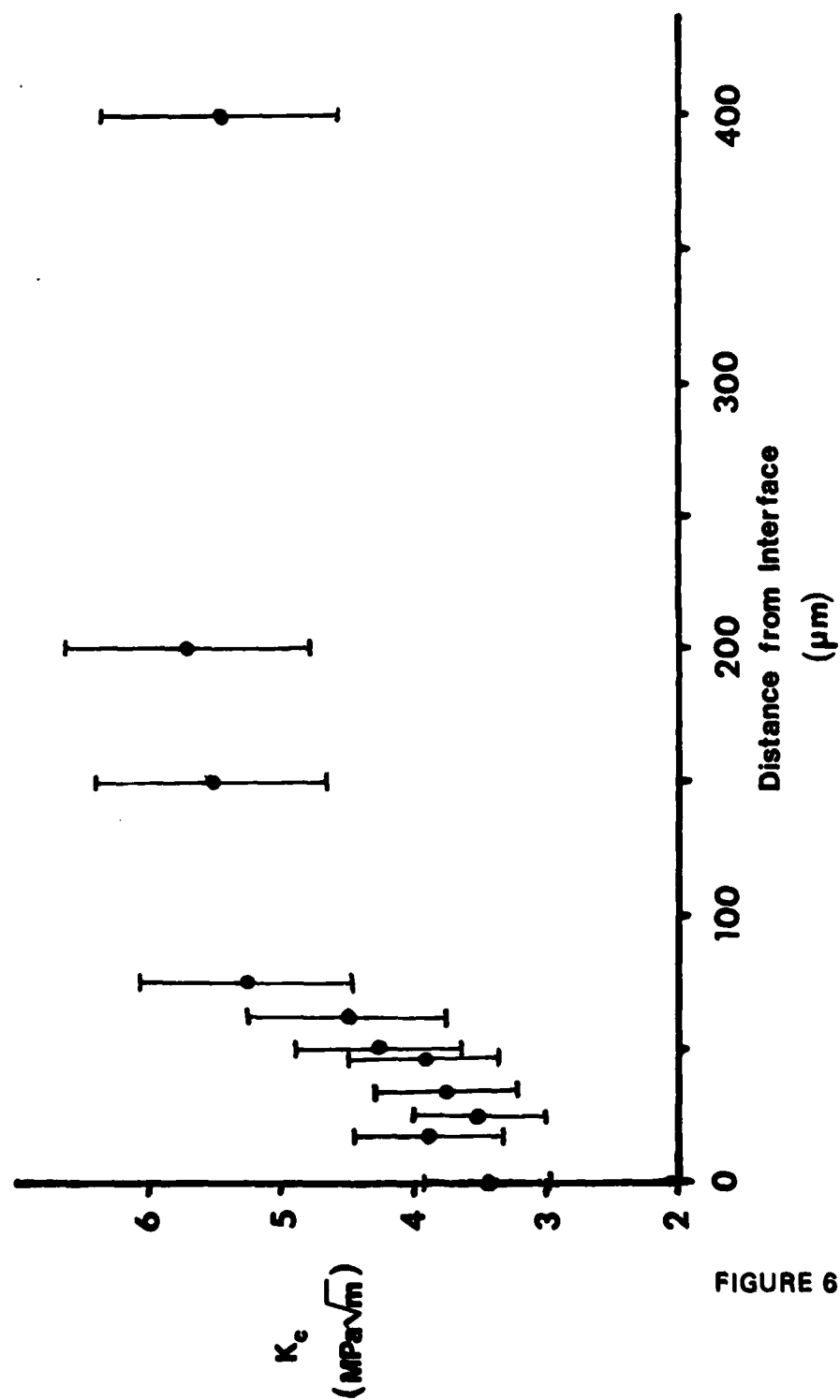


FIGURE 6

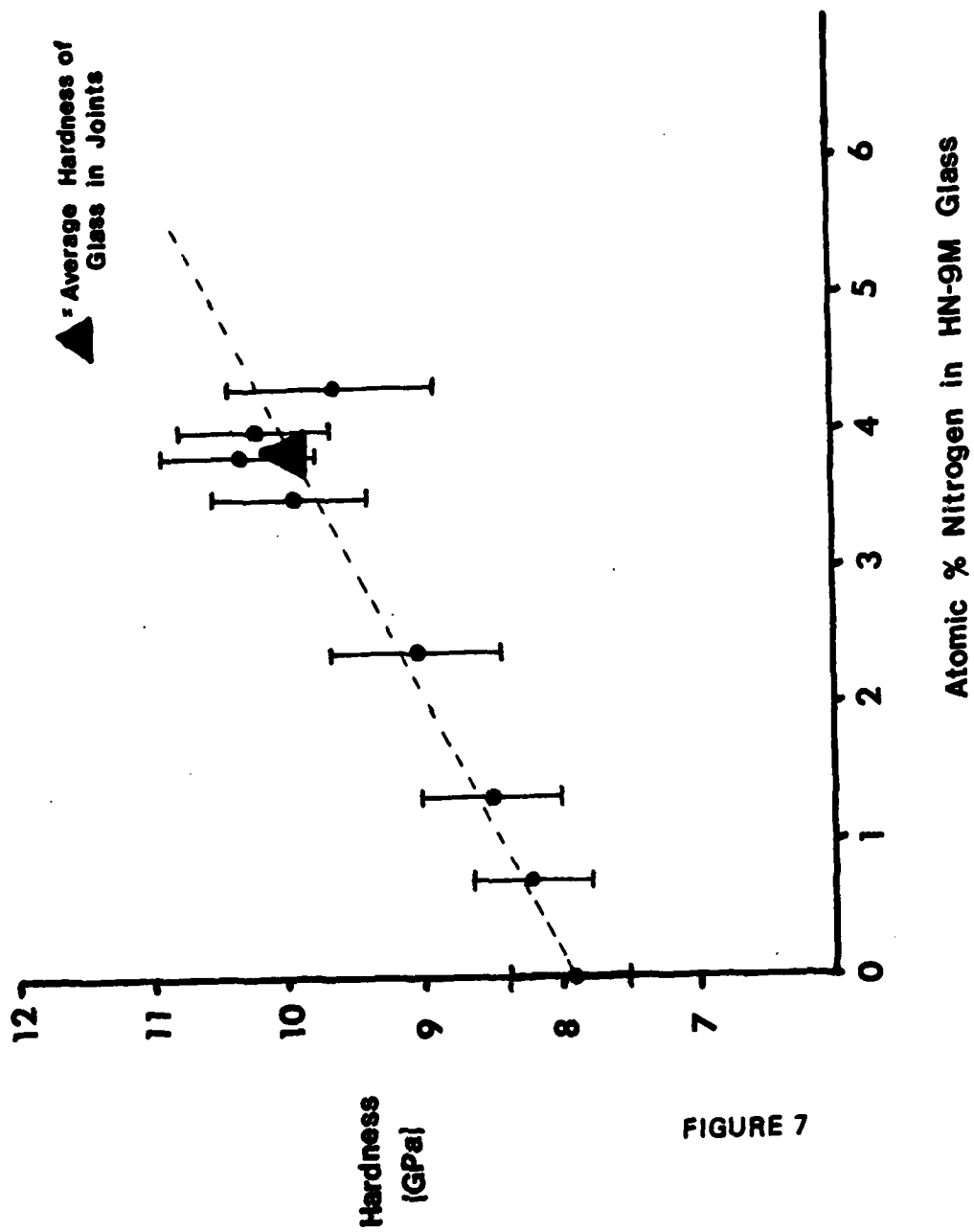


FIGURE 7

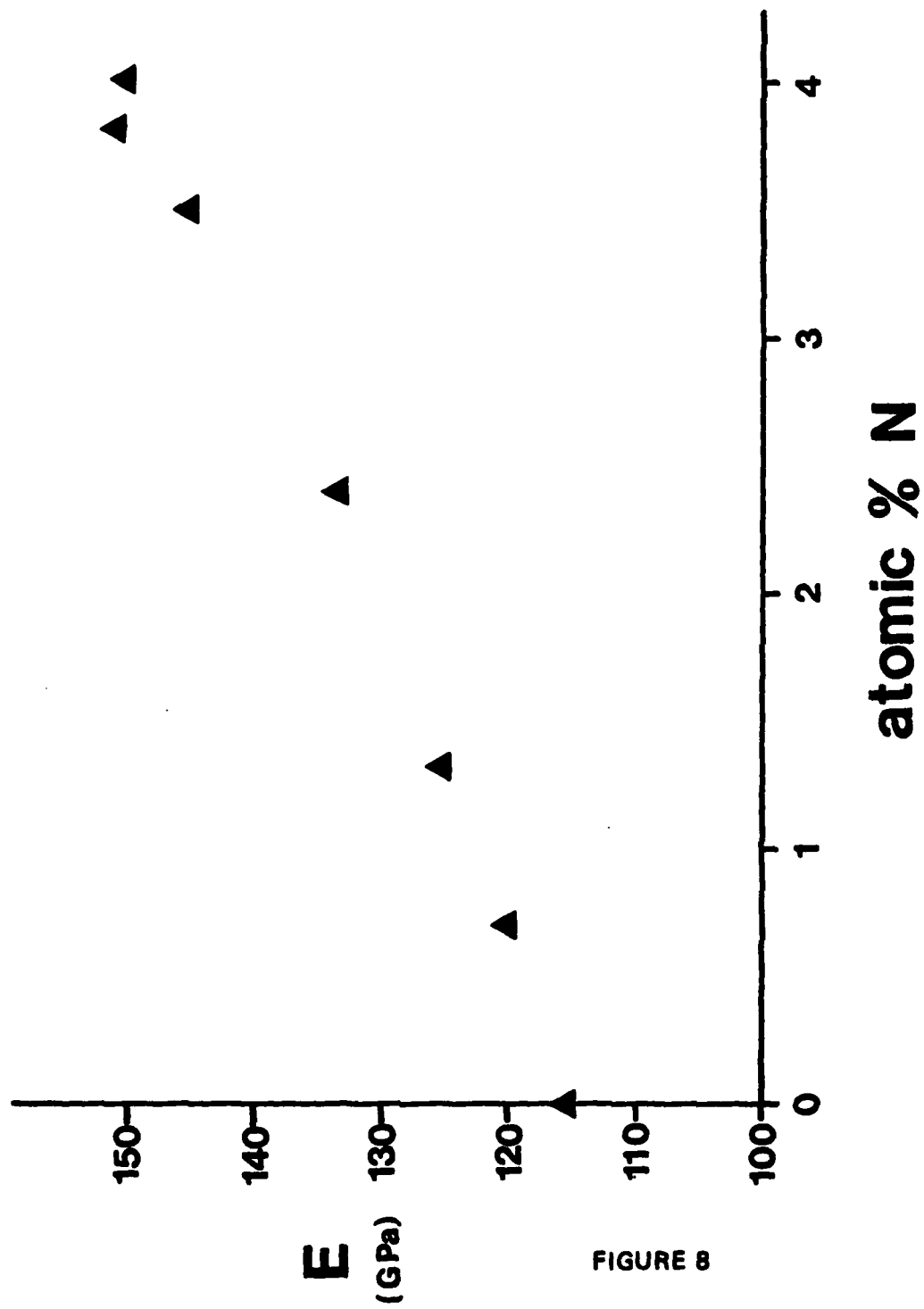


FIGURE 8

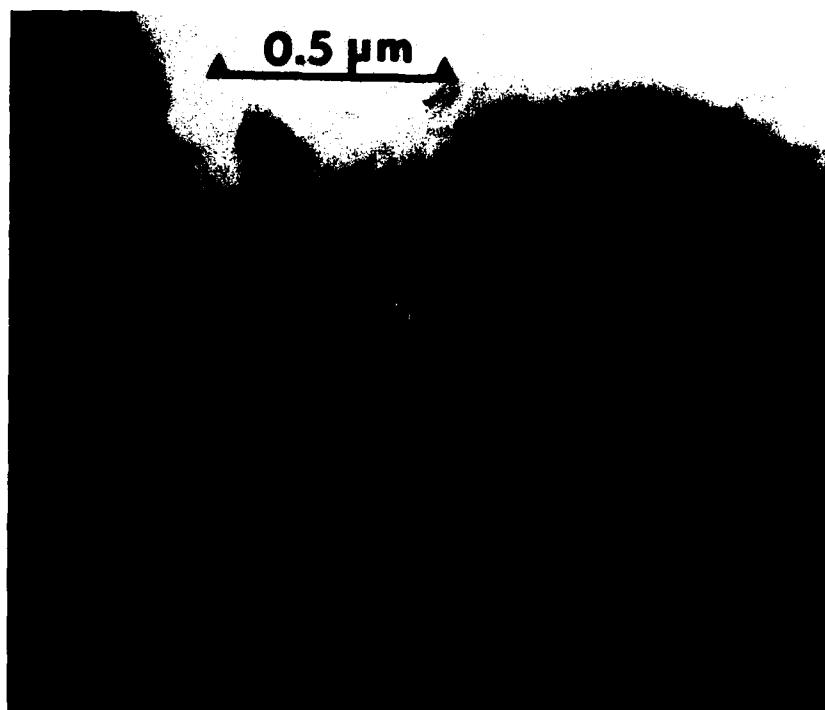


Figure 9

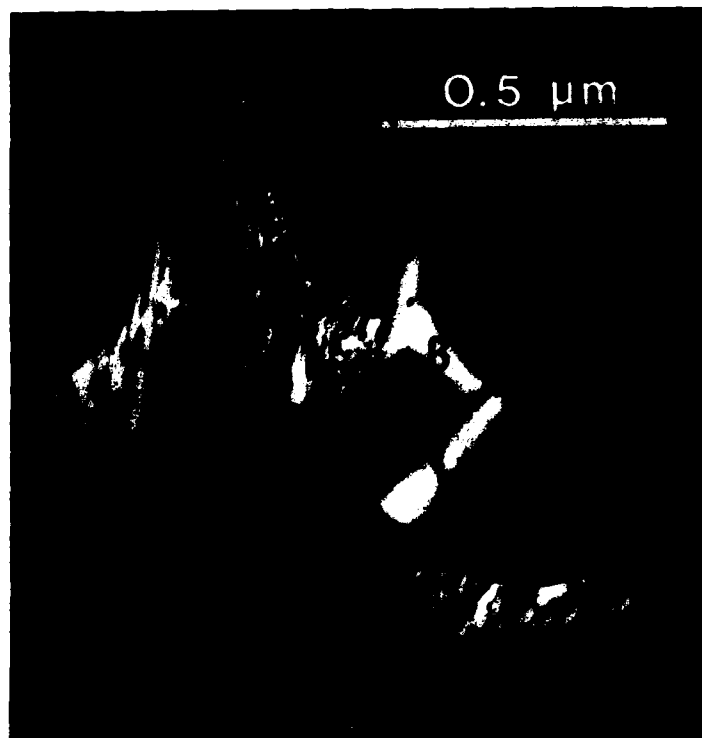


Figure 10



**END**

**FILMED**

**10-84**

**DTIC**